Naval Research Laboratory

Washington, DC 20375-5320

NRL/6043/MR--2021/1

Numerical Analysis of Gas Explosions in Coal Mines

Vadim N. Gamezo

Laboratory for Multiscale Reactive Flow Physics Branch
Laboratories for Computational Physics and Fluid Dynamics

Elaine S. Oran

Logan Kunka

Department of Aerospace Engineering
Texas A&M University
College Station, TX

Carolyn R. Kaplan

Department of Aerospace Engineering
University of Maryland
College Park, MD

March 2, 2021

REPORT DOCUMENTATION PAGE

Form Approved
OMB No. 0704-0188

1. REPORT DATE *(DD-MM-YYYY)*	**2. REPORT TYPE**	**3. DATES COVERED** *(From - To)*
02-03-2021	NRL Memorandum Report	09/01/2018 – 09/01/2020

4. TITLE AND SUBTITLE

Numerical Analysis of Gas Explosions in Coal Mines

5a. CONTRACT NUMBER
NCRADA-NRL-18-673

5b. GRANT NUMBER
AFC215FO-73

5c. PROGRAM ELEMENT NUMBER

6. AUTHOR(S)

Elaine S. Oran*, Vadim N. Gamezo, Carolyn R. Kaplan**, and Logan Kunka*

5d. PROJECT NUMBER

5e. TASK NUMBER

5f. WORK UNIT NUMBER
1F00

7. PERFORMING ORGANIZATION NAME(S) AND ADDRESS(ES)

Naval Research Laboratory
4555 Overlook Avenue, SW
Washington, DC 20375-5320

8. PERFORMING ORGANIZATION REPORT NUMBER

NRL/6043/MR--2021/1

9. SPONSORING / MONITORING AGENCY NAME(S) AND ADDRESS(ES)

Alpha Foundation for the Improvement of Mine
Safety and Health, Inc.
P.O. Box 1371
Lenoir City, TN 37771

10. SPONSOR / MONITOR'S ACRONYM(S)

11. SPONSOR / MONITOR'S REPORT NUMBER(S)

12. DISTRIBUTION / AVAILABILITY STATEMENT

DISTRIBUTION STATEMENT A: Approved for public release; distribution is unlimited.

13. SUPPLEMENTARY NOTES

*Department of Aerospace Engineering,Texas A&M University, College Station, TX 77843
**Department of Aerospace Engineering, University of Maryland, College Park, MD 20742

14. ABSTRACT

We use reactive CFD simulations to study worst-case scenarios for gas explosions in stoichiometric methane-air mixtures confined in large-scale obstructed tunnel geometries relevant to coal mines. In particular, we analyze effects of tunnel blockage ratio *br* and spacing of obstructions *L* on flame acceleration, formation of a shock-flame complex, deflagration-to-detonation transition (DDT), and resulting explosion pressures. We considered two types of obstructions: periodic obstacles placed on channel walls, and a layer of rock rubble that partially fills the channel. For channels with periodic obstacles and the channel height $d = 3$ m typical of coal mine tunnels, the minimum distance to DDT, $L_{DDT} = 28$ m, is observed for $br = 0.3$, $L/d = 0.5$. For channels with rock rubble and $d = 3$ m, the minimum $L_{DDT} = 5 – 5.5$ m is observed when the channel is completely filled with rocks. This DDT length is significantly shorter than the values computed for channels with periodic obstacles, but it corresponds to a relatively loose rock layer that may not be typical for realistic coal mine environments. Nevertheless, our results show that methane-air detonations in coal mines can develop quickly and produce reflected-shock pressures ~ 50 atm (735 psi). These detonations cannot be contained by the standard 50 psi or 120 psi seals that are designed to stop relatively slow deflagrations. In areas with a high risk of detonations, the seals should be designed to withstand the static pressure of at least 640 psi, as previously recommended by NIOSH.

15. SUBJECT TERMS

Gas explosions
Coal mines
Methane
Numerical modeling

16. SECURITY CLASSIFICATION OF:			**17. LIMITATION OF ABSTRACT**	**18. NUMBER OF PAGES**	**19a. NAME OF RESPONSIBLE PERSON**
a. REPORT	**b. ABSTRACT**	**c. THIS PAGE**			Vadim N. Gamezo
UU	UU	UU	UU	44	**19b. TELEPHONE NUMBER** *(include area code)* (202) 767-1973

Standard Form 298 (Rev. 8-98)
Prescribed by ANSI Std. Z39.18

This page intentionally left blank.

1. Executive Summary

Accidental gas explosions in coal mines are low-probability, high-impact events that can result in devastating losses of both human life and property, in addition to having a strong negative impact on the mining industry. These explosions usually occur when natural gas accumulates in mines to the point where it creates explosive mixtures with air. Once formed, the mixtures may be accidentally ignited and burn quickly, thus releasing large amounts of energy and generating high pressures. Natural gas is composed over 95% methane with at most a few percent of higher hydrocarbons such as ethane and propane.

To protect mine workers from possible methane explosions, abandoned areas are separated from active areas by concrete walls, or seals, meant to withstand the high pressures generated by explosions and prevent propagation of shock waves and flames into working areas. The primary objective of this project was to apply the previously developed numerical technology to predict parameters of natural gas explosions in coal-mine environments, and then to use the results to analyze protective seal design specifications.

In early studies sponsored by NIOSH, we demonstrated that numerical simulations can quantitatively as well as qualitatively predict the development of explosions in channels containing uniform methane-air mixtures. The explosions were evolving from ignition, to flame acceleration, to shock formation, and then to possible deflagration-to-detonation transition (DDT). In the last Alpha Foundation project, we extended the simulations to coal-mine sized systems (3 m-high channels), extended the submodel for chemical processes, the Chemical Diffusion Model (CDM), to include non-stoichiometric mixtures, and used the new CDM to predict flame acceleration and DDT in mixtures with composition gradients. We also showed that the technology can be used to analyze the efficiency of passive blast attenuators. Finally, we used the results of the simulations to analyze the adequacy of specifications for protective seal design.

The work performed for the current project had three primary objectives, which were to: (1) Examine the effects of tunnel geometries relevant to coal mines on flame acceleration and DDT by varying the tunnel blockage ratio and spacing of obstructions, including periodic obstacles and rock rubble; (2) Examine the effects of including small amounts of ethane and propane impurities in the methane, therefore better modeling actual natural gas, and (3) Analyze the protective seal design specifications in terms of the new results. Major conclusions of this work are:

1. Scaling laws describing the dependence of the distance to DDT (L_{DDT}) on the channel height (d) were extended to include the effects of varying the blockage ratio (br) and obstacle spacing (L).

For channels with periodic obstacles, L_{DDT} increases with d such that L_{DDT}/d decreases. For $d = 3$ m typical of coal mine tunnels, the minimum $L_{DDT} = 28$ m ($L_{DDT}/d \approx 9$) was observed for $br = 0.3$, $L/d = 0.5$. In addition to L_{DDT}, we also computed the distance L_{SF} at which the shock and the flame become loosely coupled and form a shock-flame complex that has a high destructive potential.

For channels with rock rubble, L_{DDT} increases and L_{DDT}/d decreases with d. Both L_{DDT} and L_{DDT}/d decrease with the increasing br, and reach the minimum when the channel is completely filled with rocks ($br = 1$). For $d = 3$ m typical of coal mine tunnels, L_{DDT} reaches $8 - 9$ m for $br = 0.4375$, and $5 - 5.5$ m for $br = 1$. This corresponds to $L_{DDT}/d \approx 3$ for $br = 0.4375$, and $L_{DDT}/d \approx 1.8$ for $br = 1$. These DDT lengths are significantly shorter than values computed for

Manuscript approved February 19, 2021.

channels with periodic obstacles, but they correspond to worst-case scenarios with relatively loose rock layers that may not be typical for realistic coal mine environments.

2. Small additions of ethane or propane to methane-air mixtures have practically no effect on the distance to DDT. L_{DDT} computed as a function of additive concentration shows some fluctuations that are no greater than the inherent stochasticity of the system.

3. Our results show that the possibility and the destructive potential of detonations in underground coal mines should not be underestimated. Detonations in near-stoichiometric methane-air mixtures contained in obstructed areas can develop quickly on scales as short as 5 m, and produce reflected-shock pressures ~ 50 atm (735 psi). These detonations cannot be contained by the standard 50 psi or 120 psi seals that are designed to stop relatively slow deflagrations. In areas with a high risk of detonations, the seals should be designed to withstand the static pressure of at least 640 psi, as previously recommended by NIOSH.

2. Problem Statement and Objective

The project is based on the solicitation focus area "Health and Safety Interventions," and the topical area is "Fire and Explosion Prevention."

Problem Statement

Accidental gas explosions in coal mines are low-probability, high-impact events that cause devastating losses of human life and property, and have strong negative impacts on industry [1-4]. These explosions can occur when natural gas (mostly methane) mixes with the background air and reaches a concentration and volume in which the mixture is easily ignitable and could explode. Such gas mixtures are more likely to form in abandoned, unventilated mining areas that may be several kilometers long. They may be ignited accidentally by sparks created by, for example, falling rocks, equipment, spontaneous coal ignition, or possibly lightning, then burn quickly, release large amounts of energy, and generate high pressures.

To protect workers and mines from possible methane explosions, abandoned mining areas are separated from active areas with concrete walls, or *seals* [5,6]. These seals must be strong enough to withstand high explosion pressures and thus prevent propagation of shock waves and flames into working areas.

In the absence of large-scale test facilities where pressures could be measured in realistic scenarios, computational models [7-18] capable of predicting details of gas explosions are the only option for determining explosion pressures. The development of computational technologies and the continuous increase in computing power that occurred in the last few decades have transformed research and development in many industries, including automotive and aerospace. Expensive series of experiments, once carried out to test and optimize new designs, are now frequently replaced by a combination of numerical simulations and a limited number of well-chosen experiments used to calibrate and validate the numerical models. This reduces costs and accelerates the development of new technologies and products. Numerical simulations of uncontrolled gas explosions are now instrumental for safety studies in many of the industries in which explosive gas-air mixtures can form, including oil and gas industries, chemical processing, power generation, and hydrogen technologies. Nuclear reactor shells and buildings are designed to withstand accidental hydrogen-air explosions or mitigate their effects, and these designs are optimized using numerical models [19-22].

In the coal mine industry, numerical simulations of gas explosions were less common, partially because the computing power required for credible simulations of explosions on large scales, which are characteristic of underground coal mines, have only recently become available. Most of the basic input data required for these simulations and the numerical techniques needed to solve the governing equations have been developed, implemented in numerical codes, tested on smaller scales, and used in other industries. In recent years, explosion simulations were used to analyze mine disasters [8] and provide guidelines for the design of protective seals [6].

Prior Results – The Basis for Current Work

Under a prior grant from the Alpha Foundation (AFC215-20), we developed a suite of numerical models to predict the effects of accidental gas explosions in coal mines. The purpose of that project was to advance current numerical simulation capabilities to the point where they give reliable estimates of pressures that can arise during a methane explosion. There were four main, interrelated tasks: (1) Demonstrate that numerical simulations can in fact predict the development of explosions

for uniform methane-air mixtures evolving from ignition, to flame acceleration, to shock formation, and to possible deflagration-to-detonation transition (DDT); (2) Extend the existing chemical-diffusive submodel for methane-air combustion so that it can predict explosions in nonuniform methane-air mixtures; (3) Demonstrate that the technology can be used to analyze the efficiency of passive blast attenuators; (4) Use results of the simulations to analyze the adequacy of specifications for protective seal design.

There were two major practical conclusions discussed in more detail in the final report to the Alpha Foundation for the prior project, *Numerical Tools for Mitigation of Methane Explosions in Coal Mines*, which was carried out from August 1, 2015 to August 1, 2017.

The first conclusion is related to the numerical technology. *As a result of this prior work, the numerical technology for gas explosion modeling was developed to the point where it can be reliably used for predicting flame acceleration, possible deflagration-to-detonation transition (DDT), and resulting pressures in large tunnels filled with methane-air mixtures and containing obstacles, which is typical of conditions that might be encountered in coal mines.*

This ability to predict flame acceleration and DDT accurately was demonstrated in a number of ways, including comparisons of simulations obtained by very different numerical algorithms and full computer codes, comparisons of results of simulations to available experimental data, derivation of scaling laws, and extensions to consider effects of rock rubble. The importance of this predictive capability extends beyond the coal-mine industry. The same computational technology can be instrumental in developing new devices for gas explosion prevention and mitigation in many industries where the risk of gas explosions exists.

The second conclusion is related to the results of computations for a worst-case scenario, methane-air at stoichiometric conditions. *Detonations can form in coal mine tunnels and produce pressure peaks at protective seals that are significantly higher than the static pressure requirements in MSHA regulations.*

Computations performed for the worst-case scenario (stoichiometric methane-air mixture in a 3-m-high tunnel with the blockage ratio 0.3) show that in a 20-m-long tunnel, a flame can accelerate enough to produce a 44 psi ($\sim$3 atm) incident shock, and the reflected-shock pressure at the seal will then exceed 120 psi ($\sim$8.2 atm).

For tunnels longer than 35 m, detonations may form and result in pressure peaks at the seal that can reach 120 atm (1764 psi) locally and 54 atm (794 psi) averaged over the seal surface. Even higher pressures can be generated when detonations form and propagate in the compressed gas behind the reflected shock. In this case, local and averaged pressures at the wall could exceed 1200 atm (17635 psi) and 300 atm (4409 psi), respectively. The highest pressures however, last only a very short time (less than a microsecond). The effects of such short, high-pressure pulses on structures are different from static loads. Understanding these effects requires an additional structural analysis of the seals, or testing the seals under explosion loads in large-scale experiments. This series of computations also showed that the distance to detonation, L_{DDT}, as a function of channel height, d, is slightly nonlinear, and this allowed us to derive scaling laws which may be used to extrapolate towards larger channel sizes. Finally, the distances to DDT for interconnected channels are shown to be only slightly longer than those for single obstructed channels, and do show a similar tendency as a function of the channel height.

Aims and Objectives of the Current Project – The Research Objective

An overriding objective of this and the prior Alpha Foundation projects was to bring the existing numerical technology needed to predict methane-air explosions in coal-mine environments to a new level with greatly expanded capabilities, and then to demonstrate its use by applying this technology to protective seal designs. The current project, as a natural continuation of prior work, includes further development of computational models and extensions of the geometric and physical complexity of the problems considered. It also includes the application of these numerical models for the assessment of seal engineering specifications.

The project had four specific objectives:

(1) To predict the development of explosions for additional tunnel geometries relevant to coal mines by varying the tunnel blockage ratio and obstacle spacing. These additional geometries will also include tunnels partially filled with rock rubble. Scaling laws will be developed for various geometries, and used to extrapolate the results on large scales. A similar approach was used in the previous project for one fixed blockage ratio and obstacle spacing.

(2) To predict the development of explosions for methane-air mixtures blended with higher hydrocarbons, such as ethane and propane. These hydrocarbons are known to decrease the chemical induction time of methane-air mixtures, and this could affect the flame acceleration and DDT. Chemical reaction models will be developed using the technique developed in the previous project.

(3) To analyze the protective seal design specifications. As part of these simulations, pressure histories at protective seals will be calculated and compared with current MSHA criteria for seal design.

There was a fourth objective, which could not be put onto a timeline: (4) To simulate scenarios explored in the experiments that were to be carried out in the new explosion test facility at the Colorado School of Mines (CSM). Events beyond all of our control delayed data availability.

3. Research Approach

The technical approach was based on numerical models and techniques developed in the framework of the previous project. These include time-dependent, multidimensional simulation tools (called FAST and ALLA) for solving the full set of reactive Navier-Stokes equations. The fluid portions of the equations are solved by high-order numerical methods. The addition of dynamically adapting computational meshes (adaptive mesh refinement) allows increased resolution when important structures evolve in the flow. This is coupled to a newly developed chemical-diffusion model (CDM) for methane-air combustion. As part of the previous project, an automated technique for finding input parameters for the CDM was created. This allowed us to generate a model valid for variable concentrations of methane in air so that the effects of concentration gradients could be assessed.

Now we have extended the CDM to include the presence of higher hydrocarbons that can appear in coal mines and increase the reactivity of methane-air mixtures, applied these models to analyze the explosion development in a variety of obstructed channel geometries typical of coal mines, and estimated the effects of these explosions on protective seals in coal mines.

The previous project included numerical studies of flame evolution in obstructed channels filled with methane-air mixtures for the blockage ratio $br = 0.3$ and the obstacle spacing equal to the channel height.

We have now extended these studies to include other blockage ratios and obstacle spacings. We have also explored channels that are partially filled with rock rubble, both because they are relevant for coal mine geometries, and because we planned to compare the results to experimental data produced by CSM.

Models and Simulations for Methane-Air Mixtures with Other Hydrocarbons

The coal bed gas that leads to explosions in coal mines is composed primarily of methane, which is the least sensitive of all hydrocarbons to ignition and has the lowest detonability when mixed with air. Other hydrocarbons that can be present in coal bed gas are more sensitive, and they are thought to have an effect on the detonability of methane-air mixtures.

The composition of natural gas is not strictly defined and varies with source. Typically it includes $82 - 99\%$ of methane by volume depending on the gas origin [23,24], as well as ethane, propane, and small amounts of higher hydrocarbons. A few percent of nitrogen and carbon dioxide can also be present. A typical coal bed gas (often called coal bed methane) is usually mostly methane with less than 2% of ethane and heavier hydrocarbons, but sometimes it may contain up to 15% of carbon dioxide [25,26].

The variability of the composition of natural gas can result in large uncertainties in explosive properties of natural gas mixtures with air. It has been shown, for example, that small additives of ethane, propane, and higher alkanes significantly decrease ignition delays in methane-oxygen and methane-air mixtures [27,23,24]. The induction length δ of a one-dimensional steady-state detonation in stoichiometric methane-ethane-air mixtures computed in [27] can be approximated as

$$\delta/\delta_0 = 1 - 13.52x + 167.5x^2 - 1370x^3 + 5846x^4 - 9625x^5 \qquad (1)$$

where $\delta_0 = 2.41$ cm is the induction length for methane-air, and $x \leq 0.2$ is the volume fraction of ethane in the methane-ethane mixture. According to this equation, 8% ethane in natural gas decreases the induction length by a factor of two.

Ignition delays or induction lengths usually correlate with both the energy required for detonation initiation and the detonation cell size, both of which characterize the detonability of the mixture. Thus, the detonability of mixtures of natural gas and air varies with the composition of the natural gas composition and can differ significantly from that of methane in air.

Thus, because the exact composition of coal bed gas depends on the source, and the effects of other hydrocarbons on accidental gas explosions in coal mines are still practically unexplored, this creates uncertainties for computations of gas explosions and comparisons to experiments.

Our goal is to reduce these uncertainties by developing models that take into account the actual natural gas composition. We consider additions of ethane (C_2H_6) and propane (C_3H_8), which are the most abundant components in coal bed gas after methane (CH_4) [25, 28-32]. The reaction modeling approach that we take is to compute sets of model parameters that reproduce laminar flame and detonation properties in uniform mixtures with various C_2H_6/CH_4 and C_3H_8/CH_4 ratios. These parameter sets are then approximated by functions of mixture composition.

We then use the resulting reaction models to compute flame acceleration and DDT in small-scale channels and explore the effects of mixture composition. The results are compared with existing experimental data for methane-air mixtures. To extend these results to larger scales, it is important to establish scaling laws for flame acceleration and DDT in blended methane-air mixtures and to relate them to known effects of scales in pure methane-air mixtures.

The Worst Case Scenario

In the simulations performed for this study, we frequently refer to the "worst-case scenario," the conditions for which the mixture composition and channel geometry result in DDT occurring at shortest distances from the ignition point, thus producing the highest pressures. This scenario usually involves near-stoichiometric mixtures that have the highest reaction rates and energy density, and provides the upper limit on the pressure loads to which protective seals may be subjected.

Specific Objectives and Tasks of the Research

Objective 1: To predict the development of explosions for pure methane-air mixtures.

1.1. Compute flame acceleration and DDT for single obstructed channels of various heights using existing models. Vary blockage ratio and obstacle spacing. Compare the results with experimental data produced at CSM (if available).

1.2. Compute flame acceleration and DDT for single channels of various heights partially filled with rock rubble. Vary the height and porosity of the rock layer, and the rock sizes. Compare the results with experimental data produced at CSM.

1.3. Determine scaling laws based on experimental and numerical results. The scaling laws should provide distances to DDT for configurations considered in Tasks 1.1-1.2 as functions of channel height. Evaluate the largest scales that can be computed directly.

1.4. Apply calibrated models to larger scales typical of coal mine tunnels. "Apply" here means either compute large-scale configurations directly, or use scaling laws to extrapolate results obtained on smaller scales. The values that need to be extrapolated are distances to DDT and the duration of maximum pressure pulse at the end wall.

Objective 2: To predict the development of explosions for methane-air mixtures blended with higher hydrocarbons: C_2H_6 and C_3H_8.

2.1. Develop and calibrate chemical-diffusion models applicable to both deflagrations and detonations in methane-air mixtures with additives (one additive at a time). The model must reproduce distances to DDT measured in experiments with additives (if available), and a qualitative behavior of flames and detonations in mixtures observed in experiments.

2.2. Compute flame acceleration and DDT in mixtures with additives for single obstructed channels, and compare the results to pure methane-air mixtures. The comparison should show whether additives can reduce the distances to DDT, and how this effect depends of the additive concentration. The computations and analysis will be performed for small scales.

2.3. If the results of 2.2 show that additives can significantly reduce distances to DDT, extrapolate these distances to larger scales typical of coal mines.

Objective 3: To analyze the protective seal design specifications

3.1. Compute the effect of gas explosions on protective seals by modifying the downstream boundary used in calculations for objectives 1 and 2 to simulate a solid wall. Each simulation will record the pressure history at the end wall. The computed pressure histories will be compared to the current MSHA criteria for seal design.

The timeline that was followed for this work is shown below in Table 1.

Table 1. Program plan expressed as a Gantt chart.

	Year 1				Year 2			
	Q1	Q2	Q3	Q4	Q1	Q2	Q3	Q4
Objective 1: **Pure methane-air mixtures**								
1.1 Channels with obstacles		*						
1.2 Channels with rock rubble				*				
1.3. Determine scaling laws						*		
1.4 Apply models for large scales								*
Objective 2: **Blended Mixtures**								
2.1 Develop and calibrate models				*				
2.2 Apply model to small scales						*		
2.3 Extrapolate results to large scales								*
Objective 3: **Seal design specifications**								
3.1 Compare results to MSHA specs								*

(*) Milestones correspond to the completion of each task

Personnel working on the computational program included:

Dr. Vadim Gamezo, US Naval Research Laboratory
Dr. Carolyn Kaplan, University of Maryland
Dr. Elaine Oran, Texas A&M University and University of Maryland
Mr. Logan Kunka, graduate student at Texas A&M University
Mr. Christian Bachman, formerly graduate student, University of Maryland.

4. Research Findings and Accomplishments

Objective 1: To predict the development of explosions for pure methane-air mixtures.

Task 1.1. Compute flame acceleration and DDT for obstructed channels with fixed heights using existing models. Vary blockage ratio and obstacle spacing.

Channels with periodic obstacles are often used to study flame acceleration and DDT in experiments and are also typical for various types of industrial facilities. On a large scale, this geometry allows us to model the flame acceleration and DDT in coal mine tunnels, which is the main motivation for this study.

We considered stoichiometric methane-air mixtures with the channel geometry shown in Figure 1. For all of the simulations, the upper boundary was considered as a symmetry plane in the channel, the left and bottom boundaries were solid walls, and the right boundary was open. The flame was ignited in the middle of the left boundary. Relevant parameters for this study are the channel height, d, the obstacle height, h, the blockage ratio, $br = 2h/d$, and the spacing between obstacles, L. The geometric parameters for all of the cases simulated are summarized in Table 2.

Computations of flame acceleration and DDT in obstructed channels were performed using two reactive fluid dynamics codes, ALLA and FAST. These codes and models have been extensively tested in the framework of the previous project. Detailed analysis of test cases showed that they produce similar results for flame-acceleration and DDT simulations. This is the case even when there are considerable differences in numerical algorithms used to solve the governing equations, as long as the input for the chemical submodel is the same. Some of the cases listed in Table 2 were computed with both codes as we continued to test the validity of using either ALLA or FAST for the simulations.

Table 2. Blockage ratios and obstacle spacings for computed cases.
Key: A – computed with ALLA. F – computed with FAST.

br	L/d =	0.5	1.0	1.5
0.3		A	A/F	A/F
0.5		A	A	A/F
0.7		A/F	A/F	A

There are two important global quantities that were computed for each case. The first is the location at which the detonation first forms, called the run-up distance, L_{DDT}. The second quantity is L_{SF}, the location at which a shock-flame complex is formed. This complex includes the leading shock and the deflagration following it at a quasi-steady separation distance considerably larger than the very small detonation wave thickness. The formation of this complex is often, but not always, a precursor to the detonation. Because not all of the cases studied result in DDT, L_{SF}, is used to characterize these configurations that do not lead to DDT. Both L_{DDT} and L_{SF} are summarized in Figure 2 as functions of the channel height d for all computed cases.

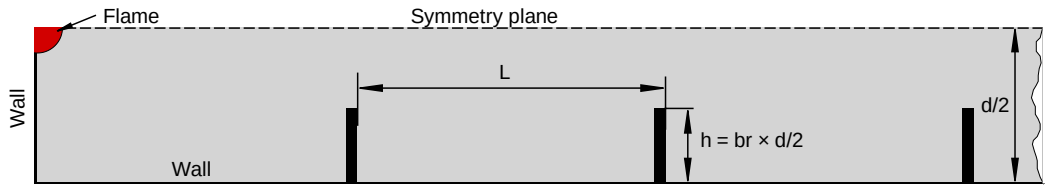

Figure 1. Computational setup.

Figure 2. (Below and next page) Distances to DDT L_{DDT} ($\diamond$) and to the formation of the shock-flame complex L_{SF} ($+$) as functions of channels height d for various blockage ratios br and scaled distances between obstacles L/d. Dashed line corresponds to the reference case $br = 0.3$, $L/d = 1$ computed previously.

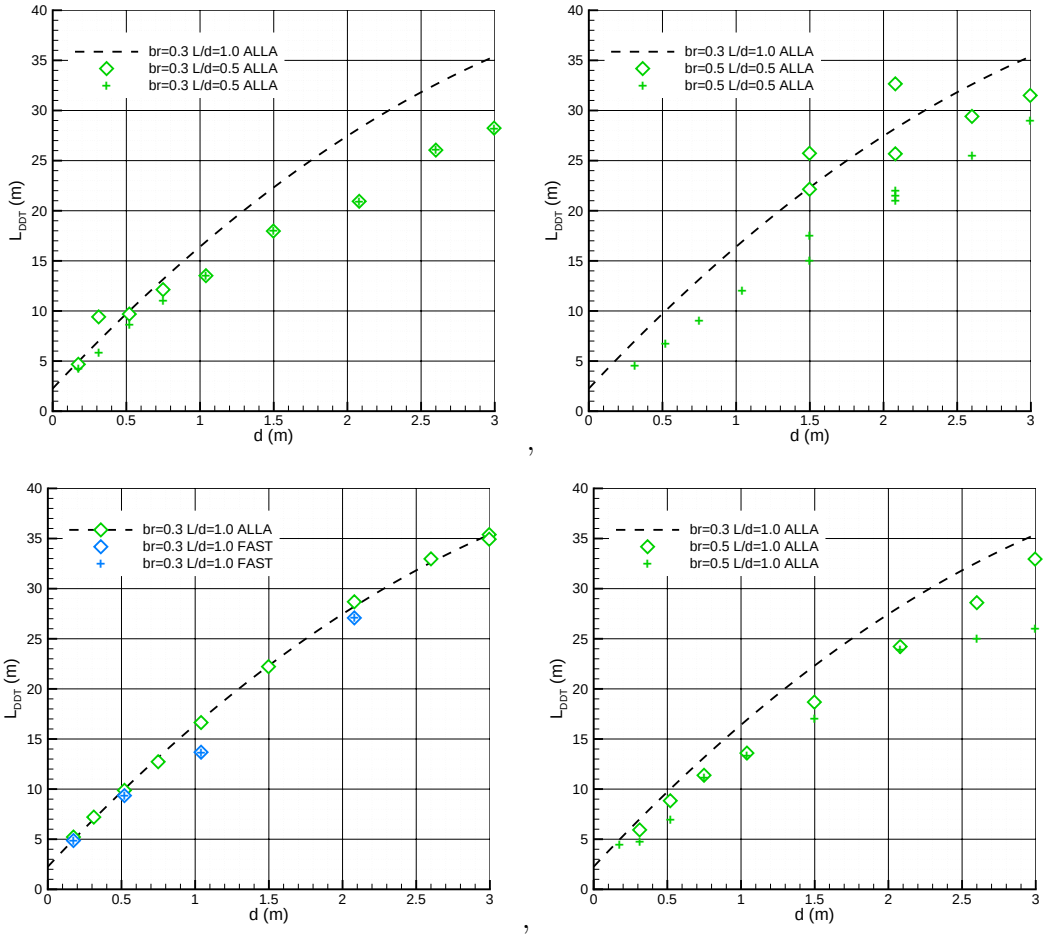

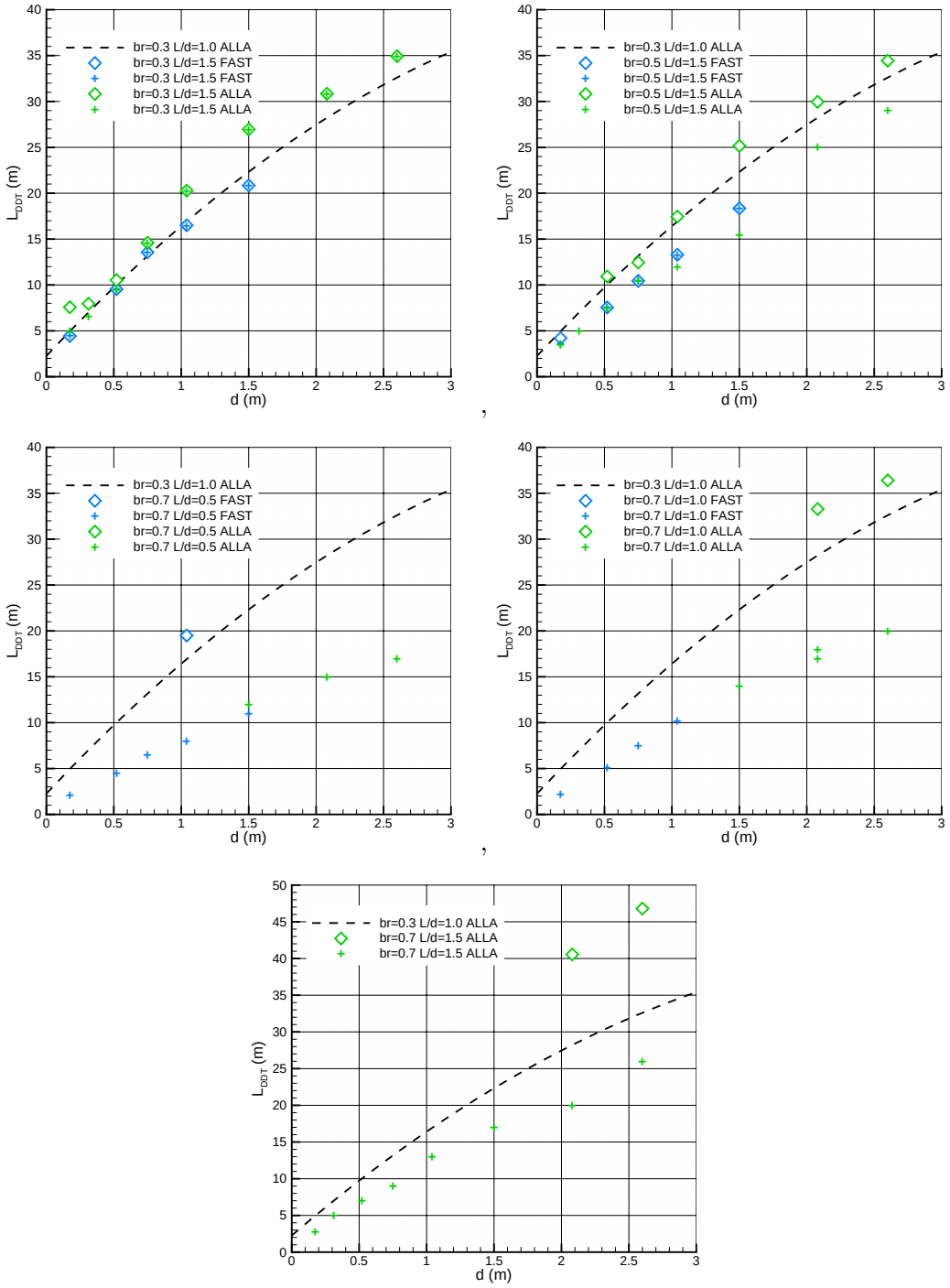

The results of simulations show two main effects of blockage ratio br and scaled distance between obstacles L/d. On one hand, the increase of br and decrease of L/d promote flame acceleration and reduce L_{DDT}. On the other hand, some configurations with higher br and smaller L/d *actually prevent detonation development*, even though local detonations may form in isolated pockets of unburned material between obstacles. This effect also depends on the channel height. For br=0.7,

for example, the detonations do not form in channels below 2 m for $L/d = 1.5$ m and $L/d = 1.0$, and do not form even in larger channels for $L/d = 0.5$. We did observe the transition to a detonation in one simulation for $br = 0.7$, $L/d = 0.5$, $h = 1$ m. Though this is rather an exception related to the stochastic nature of DDT, it shows that once the isolated detonations begin to form between obstacles, their spread to the whole system cannot be excluded.

An example of isolated detonation can be seen in Figures 3, which shows a detonation forming locally in an isolated pocket of unburned material between obstacles for the case $br = 0.5$, $L/d = 0.5$, $d = 104$ cm. An enlargement of one of the frames from Figure 3 is shown in Figure 4.

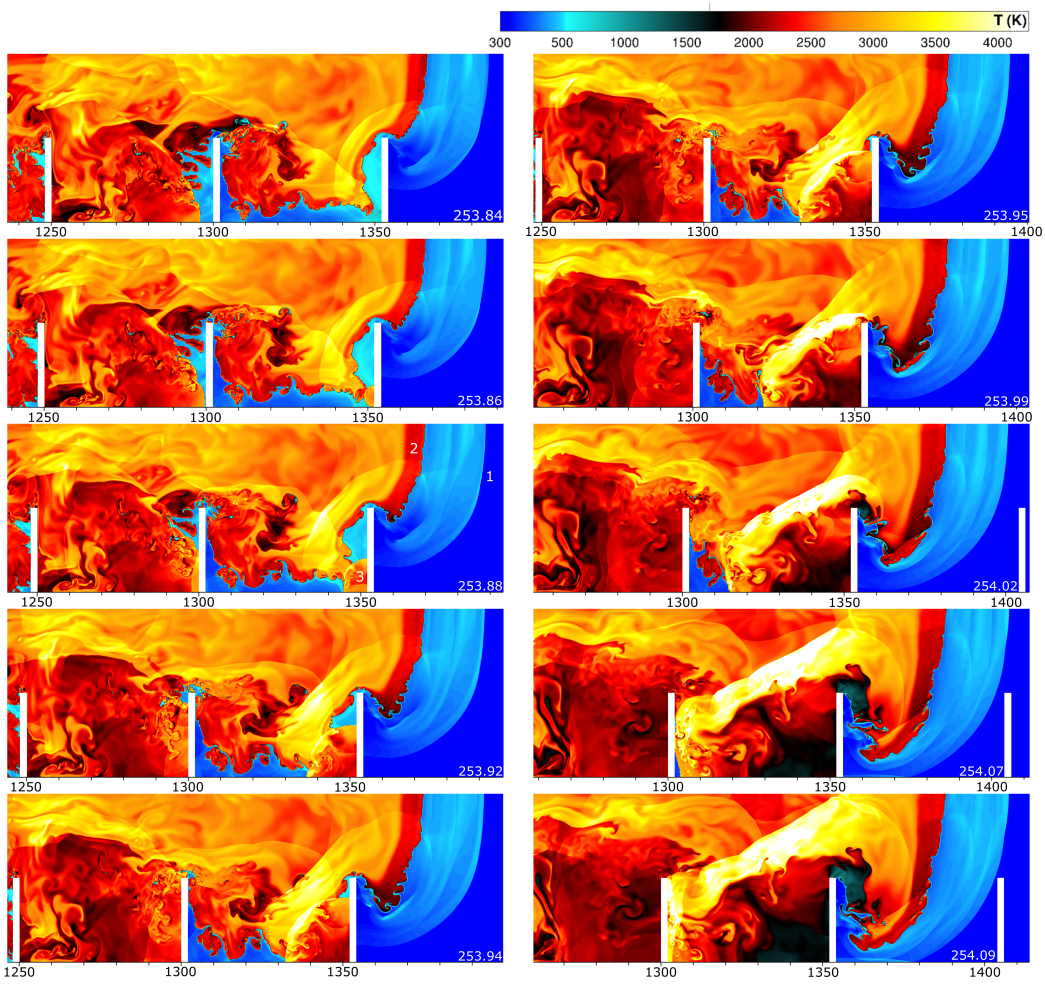

Figure 3. Development of isolated detonations between obstacles behind the leading shock and the leading edge of the flame for $br = 0.5$, $L/d = 0.5$, $d = 104$ cm. Channel positions are given in cm and time in ms.

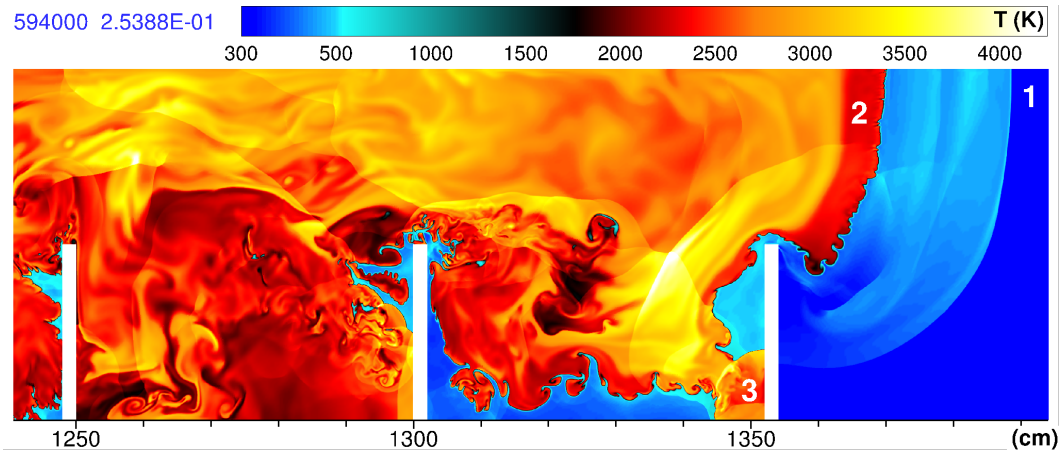

Figure 4. Enlargement of the frame showing the isolated detonation between obstacles behind the leading shock and the leading edge of the flame. 1 – the leading shock; 2 – leading flame front; 3 – detonation.

Such local detonations, which occur behind the leading edge of the flame, have no way to spread downstream because the burned material closes the gap above the obstacle before the detonation reaches it. Strong shocks produced by the isolated detonation reflect from obstacles and channel walls, diffract around the obstacle, and weaken considerably, but they do catch up and overtake the leading edge of the flame, participate in the shock collisions in the next space between obstacles, and contribute to leading shock strength. As a result, the leading shock and the turbulent flame never merge and continue to propagate as a quasi-steady-state shock-flame complex. These quasi-steady-state regimes can propagate indefinitely in relatively small channels, but eventually transition to detonations in larger channels

The results for $br = 0.5$, $L/d = 0.5$ show, for example, that for larger channels, starting from $d = 1.5$ m, detonations eventually spread and overtake the leading edge of the flame at some distance L_{DDT} that can be significantly longer than L_{SF}. Between L_{SF} and L_{DDT}, the flame and shock continue to propagate with an almost constant velocity as a quasi-steady-state shock-flame complex with isolated detonations behind. These processes are shown in more detail in a computer-generated movie of a simulation that was provided to the Alpha Foundation.

Task 1.2. Compute flame acceleration and DDT for single channels of varying heights and partially filled with rock rubble. Vary the height, porosity of the rock layer, and the rock sizes.

We modeled rock rubble with a regular array of square obstacles oriented at 45° to the channel walls and placed at the bottom part of the channel, as shown in Figure 5. The height of the rock layer h and the channel height d define the blockage ratio, $br = h/d$. The obstacle size r and spacing s define the porosity (volume fraction of voids) $pr = 1 - (r/s)^2/4$. The channel is filled with a stoichiometric methane-air mixture at initial temperature $T_0 = 298$ K and initial pressure $P_0 = 1$ atm. The mixture is ignited by spherical flames placed near the near the closed end of the channel, as shown in Figure 5. The computations are performed using an adaptive mesh with a hierarchy of cell sizes between dx_{min} and dx_{max}.

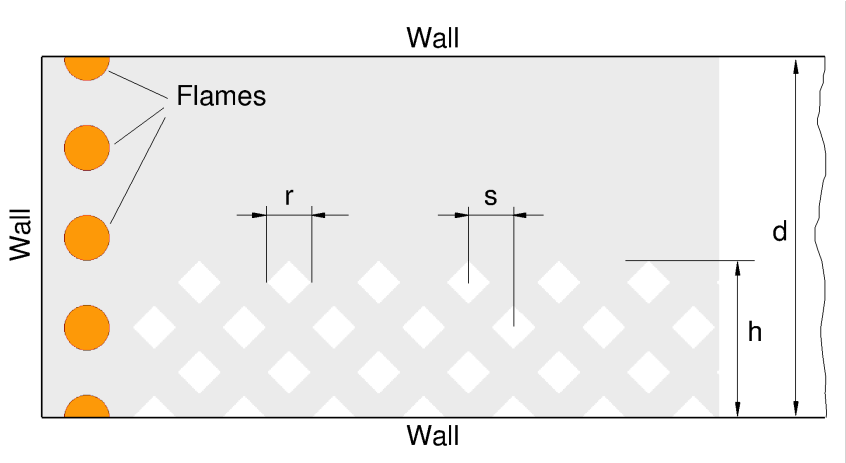

Figure 5. Computational setup. The channel and obstacle array extend to the right for many d as needed for a detonation to develop.

As the reactive mixture begins to burn, the expanding combustion products push the unreacted gas away from the closed end of the channel, and this generates a flow ahead of the flame. The flame spreads with this nonuniform flow above the rock layer and between the obstacles, and develops a very convoluted surface. This results in an increase in the burning rate, flame acceleration, and eventually a transition to a detonation at some distance, L_{DDT} from the closed end of the channel. Detonations usually appear between obstacles, as shown in Figure 6, and then spread to the space above the rocks.

Simulations of flame acceleration and DDT for various channel and rock sizes, blockage ratios, and rock spacings were carried out to evaluate the effects of these parameters on the distance to DDT. All of the cases show basically the same mechanisms of flame acceleration and DDT, with some variations of flame shapes during the flame evolution. Due to the stochastic nature of DDT, however, L_{DDT} can vary when multiple simulations are performed with what seems to be negligibly small differences. In these cases, we trigger and observe the stochastic response by changing the channel length or initial temperature by 0.001K. When all of the input parameters are exactly the same, however, the numerical solution remains deterministic, and can be exactly reproduced in repeated simulations.

Figure 7 shows the effect of channel height on L_{DDT}. We simultaneously varied d, h, r, s, along with the radius and spacing of initial flames, thus scaling the geometry shown in Figure 5 with d, and keeping the blockage ratio and porosity constant. Points of different colors and shapes correspond to different numerical resolutions, and show no systematic effect of resolution on L_{DDT}. The scatter of points in Figure 7 shows the stochastic variations of L_{DDT} within a range of a few d. This is comparable to what we observed earlier in channels with periodically placed obstacles, but L_{DDT} in channels with rubble is significantly shorter that in channels with obstacles, so the relative scatter $\delta L_{DDT}/L_{DDT}$ is larger for channels with rubble. Despite the scatter, there is a distinctive trend in which L_{DDT} increases with d. The ratio L_{DDT}/d, however, decreases with d, and becomes 3-4 for $d = 1 - 2$ m.

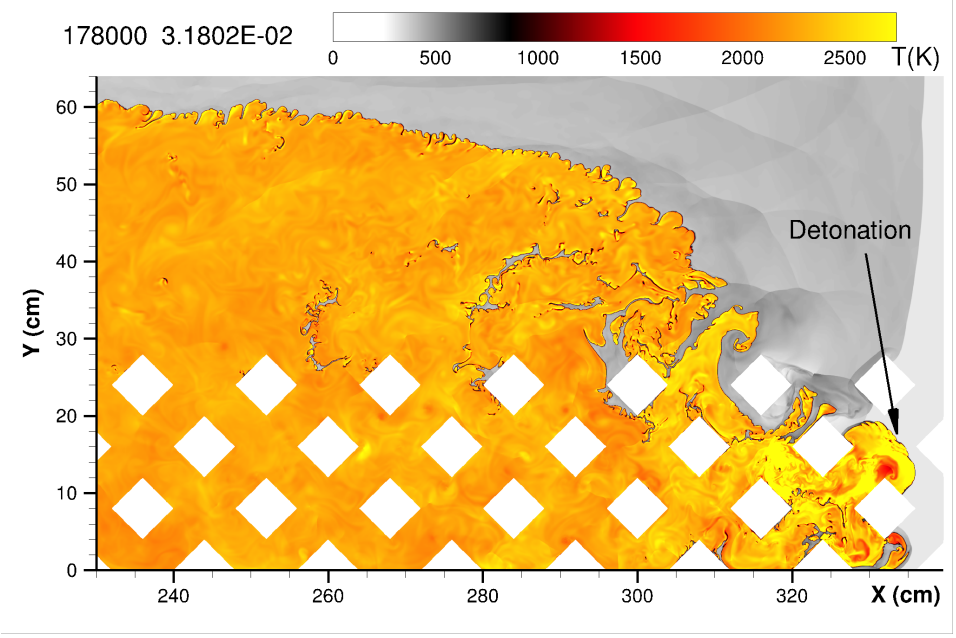

Figure 6. Flame propagation and DDT in a 64 cm channel with rock rubble at one time. The time step and the physical time (ms) are shown in the upper left corner.

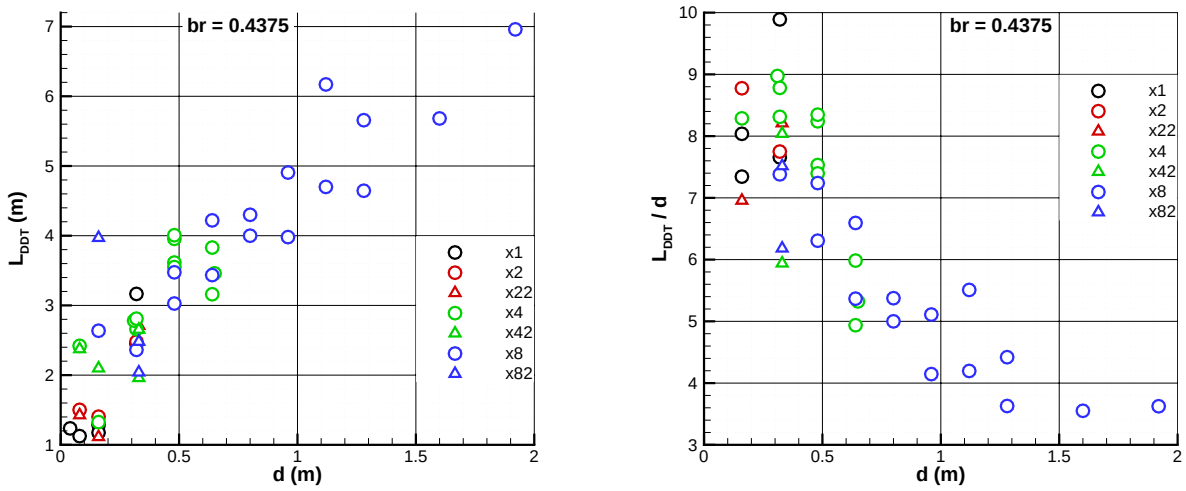

Figure 7. Absolute (left) and scaled (right) distance to DDT as a function of channel height. Points of different colors correspond to different dx_{min} (black 1/128 cm, red 1/64 cm, green 1/32 cm, blue 1/16 cm). Points of different shapes correspond to different dx_{max} (circle 1/8 cm, square 1/4 cm). The same points at the same d are produced by simulation with different channel lengths or slightly different initial T_0 to trigger the stochastic response. $br = h/d = 0.4375$, $r/d = s/d = 0.125$.

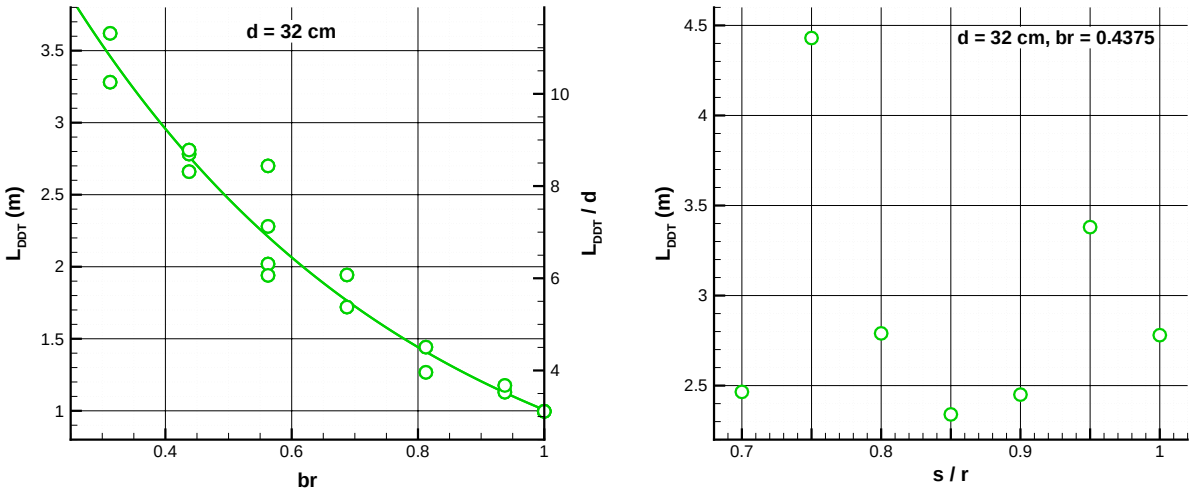

Figure 8. Distance to DDT as a function of blockage ratio (left) and porosity (right).

Figure 8 (left) shows the effect of blockage ratio on L_{DDT}. We varied h while keeping constant $d = 32$ cm, $r = s = 4$ cm. As br increases, the distance to DDT monotonically decreases, and reaches the low value of $L_{DDT}/d = 3$ when the channel is completely filled with rocks ($br = 1$).

We also varied the porosity of rock layer by changing s while keeping constant $d = 32$ cm, $h = 14$ cm, $r = 4$ cm. The resulting L_{DDT} presented in Figure 8 (right) do not show any systematic effects of porosity. When the channels between rocks become too thin (less than about 1 cm), the flame remains mostly above the rock layer, and does not produce DDT.

In realistic coal mine environments, the structure of rock rubble may vary, and on average tends to be fairly compact. If this structure does not contain interconnected voids or long irregular channels wider than ~ 1 cm, the rock layer will not promote flame acceleration. One or a few of these channels, however, can significantly increase flame speeds and explosion pressures, and this may lead to DDT. For worst-case scenarios with relatively loose rock layers that contain multiple long chains of interconnected voids wider than ~ 1 cm, the actual porosity (volume fraction of voids) of rock layer does not significantly affect the distance to DDT, which is shown in the right panel of Figure 8.

The results of simulations of flame propagation and DDT in channels with rock rubble led to recommendations for an initial set of experiments at CSM. An actual comparison of the simulations to experiments can now be performed when experimental data become available.

Task 1.3. Determine scaling laws based on experimental and numerical results. The scaling laws provide L_{DDT} for configurations considered in Tasks 1.1 and 1.2 as functions of channel height. Evaluate the largest scales that can be computed directly. This is done for (a) channels with obstacles and (b) channels with rocks.

(a) Channels with obstacles.

We focus on the two-dimensional channel geometry shown in Figure 1 and described in Task 1.1. Again, the channel contains the stoichiometric methane-air mixture that represents the worst-case scenario, and ignition occurs at the symmetry plane in the middle of the left boundary. Uniformly spaced obstacles are distributed along the channel length. Relevant parameters for this study are the channel height, d, the obstacle height, h, the blockage ratio, $br = 2h/d$, and the spacing between obstacles, L. We vary br and L, and study the effect of scale d on the distance to DDT L_{DDT} and the distance L_{SF} at which the shock-flame complex forms.

The distance L_{SF} corresponds to the point where the x-t trajectories of flame and shock become parallel, as shown in Figure 9. The shock-flame complex that forms at this point is shown in Figure 10. It consists of a strong shock, a thick compressed layer of unburned material behind it, and a flame that propagates at distance $\sim d/4$ behind the shock. The flame actively generates weaker shocks and pressure waves that catch up with the leading shock and strengthen it. Even though the leading shock pressure remains lower than detonation pressures, the destructive potential of a shock-flame complex is very high. The collision of this complex with the end wall or other solid structures generates high pressures and strong reflected shocks that can ignite a detonation. This detonation propagates in a shock-compressed material and results in extremely high wall pressures exceeding wall pressures produced by a regular detonation by a factor of 5-10 [33]. Thus, the distance L_{SF} at which the shock-flame complex forms provides an important measure of a destructive potential for a particular reactive mixture and channel geometry. This is especially relevant for channels with high br where L_{SF} can be significantly shorter than L_{DDT}.

The distances L_{DDT} and L_{SF} computed using two different codes ALLA and FAST for various geometric parameters are shown in Figure 2. Some of the cases (fixed br and L/d) were computed for channel heights up to 3 m. Other cases were computed up to 2.6 m, and the results can be extrapolated to 3 m. We summarize these data in Figure 11 using scaled distances L_{DDT}/d and L_{SF}/d.

These data show that for fixed br and L/d, both L_{DDT} and L_{SF} increase nonlinearly with d in such a way that L_{DDT}/d and L_{SF}/d decrease. For example, the reference case $br = 0.3$, $L/d = 1$ shows $L_{DDT}/d \approx 30$ for $d = 0.174$ m, and $L_{DDT}/d \approx 12$ for $d = 3$ m. For the maximum computed channel height 3 m, and the range $br = 0.3 - 0.7$ and $L/d = 0.5 - 1.5$ that we explored, the minimum $L_{DDT} = 28$ m was observed for $br = 0.3$, $L/d = 0.5$, and the minimum $L_{SF} = 18$ m was extrapolated for $br = 0.7$, $L/d = 0.5$. These distances are relevant for coal mine tunnels that have typical sizes ~ 3 m and can contain explosive methane-air mixtures. This material is discussed in publications [34, 35].

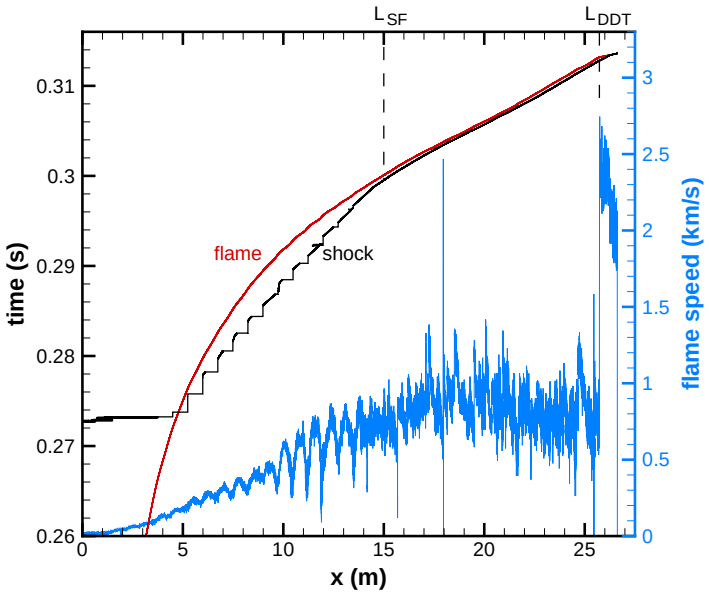

Figure 9. The x-t trajectories of the flame and shock, and the flame speed for the case $d = 149.76$ cm, $h = 37.44$ cm, $L = 74.88$ cm, $br = 0.5$, $L/d = 0.5$. L_{SF} shows the distance where the shock-flame complex forms. L_{DDT} shows the distance where the detonation forms.

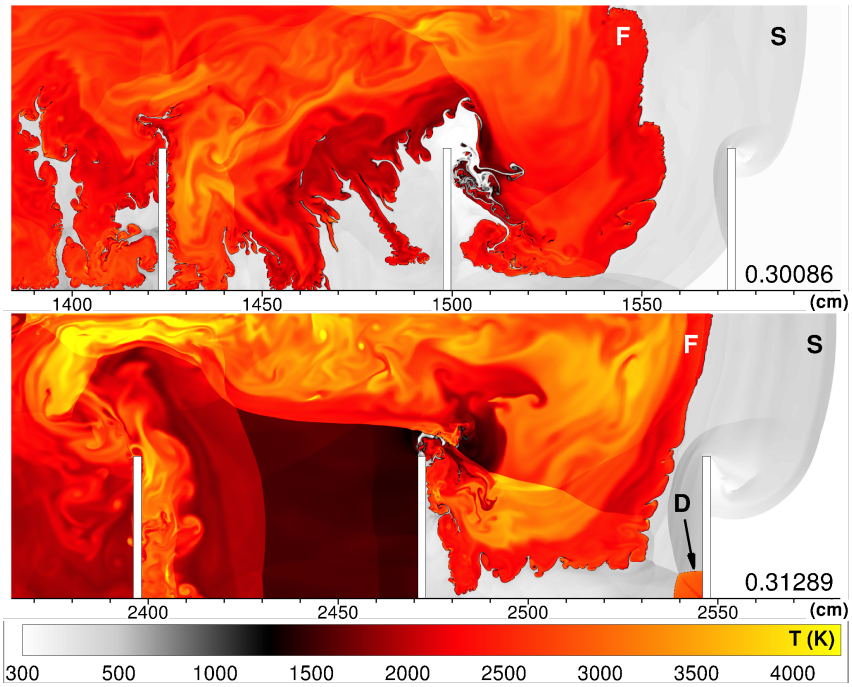

Figure 10. The temperature fields showing the shock (S) - flame (F) complex, and the formation of a detonation (D). Frames correspond to L_{SF} and L_{DDT} in Fig. 2. Time in seconds is shown in each frame. $d = 149.76$ cm, $h = 37.44$ cm, $L = 74.88$ cm, $br = 0.5$, $L/d = 0.5$.

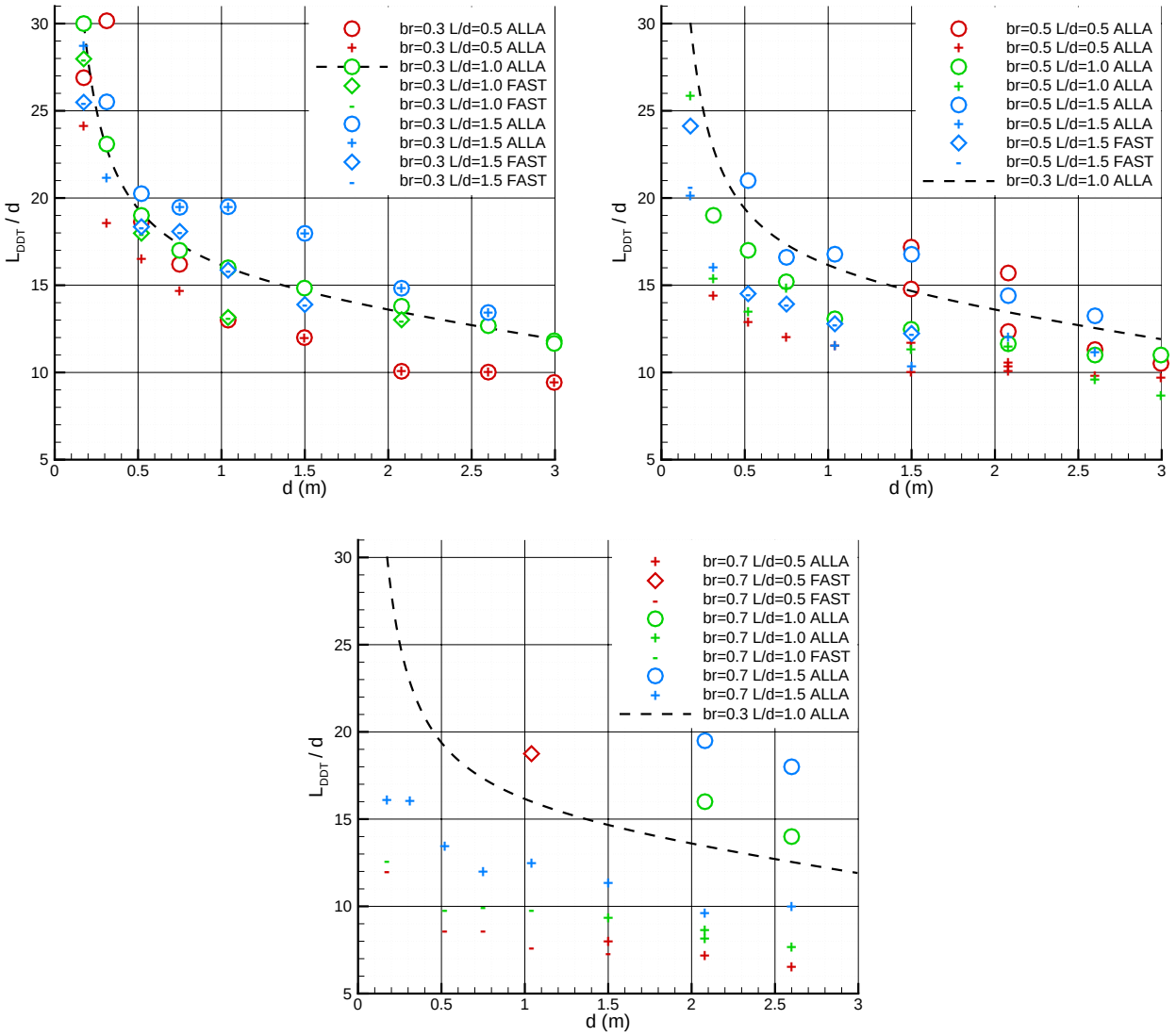

Figure 11. Scaled distances to DDT ($\circ, \diamond$) and to shock-flame complex (+, -) as functions of channel height for different blockage ratios $br = 0.3$ (left), 0.5 (right), and 0.7 (bottom). Points of different colors correspond to different obstacle spacing $L/d = 0.5$ (red), 1.0 (green), and 1.5 (blue). Points of different shapes are produced by different codes ALLA ($\circ$, +) and FAST ($\diamond$, -). The dashed line in each panel corresponds to the reference case $br = 0.3$, $L/d = 1$. For all cases, $dx_{min} = 0.065$ cm, $dx_{max} = 0.26$ cm.

(b) Channels with rock rubble. We now consider flame acceleration and DDT in channels filled with rock rubble, which is often present in coal mine tunnels and gob areas. The geometric configuration is the same as described in Figure 5.

In the material presented above, we described simulations of flame acceleration and DDT for $br = h/d = 0.4375$ and various channel sizes up to $d = 1.92$ m. We also studied the effect of blockage ratio for $d = 32$ cm. Now we have extended these simulations to larger channels up to $d = 3.2$ m while considering a range of blockage ratios between $br = 0.4375$ and $br = 1$. The resulting L_{DDT} are summarized in Figure 12. The stochastic effect is relatively small when the channel is completely filled with rocks ($br = 1$), and increases as the blockage ratio decreases. Despite the stochastic variations, there is a distinctive trend of L_{DDT} increasing with d. For $d = 3$ m typical of coal mine tunnels, L_{DDT} reaches 8-9 m for $br = 0.4375$, and 5-5.5 m for $br = 1$. The ratio L_{DDT}/d decreases with d, and becomes ~3 for $d = 3$ m and $br = 0.4375$, and ~1.8 for $d = 3$ m and $br = 1$.

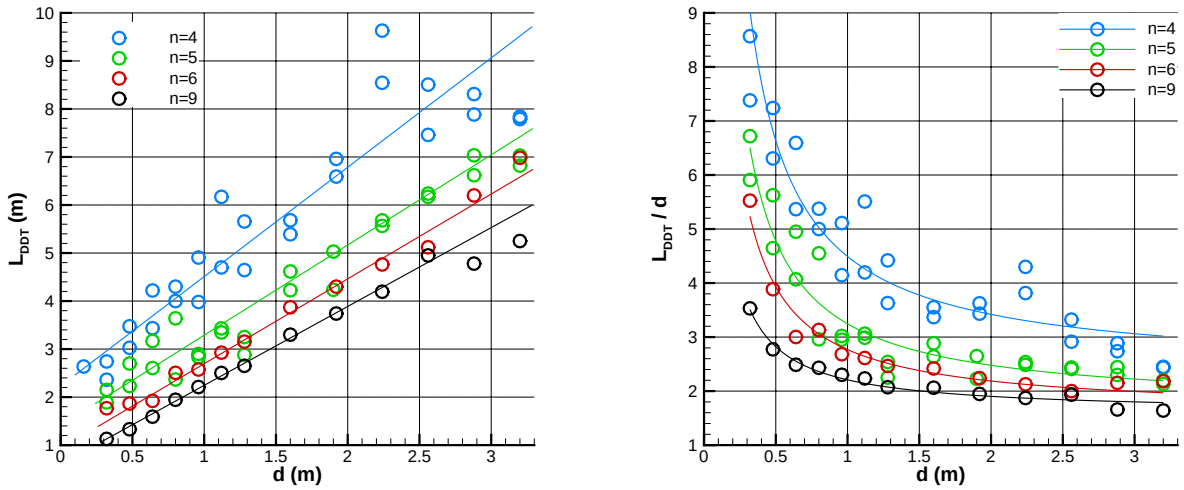

Figure 12. Absolute (left) and scaled (right) distance to DDT as a function of channel height. Points of different colors correspond to different numbers of obstacle rows n that define blockage ratios $br = h/d = 0.4375$ ($n = 4$, blue), 0.5625 ($n = 5$, green), 0.6875 ($n = 6$, red), and 1 ($n = 9$, black). The same points at the same d are produced by simulation with different channel lengths or slightly different initial T_0 to allow us to evaluate the stochastic response. $r/d = s/d = 0.125$, $dx_{min} = 1/16$ cm, and $dx_{max} = 1/8$ cm.

Task 1.4. Apply calibrated models to larger scales typical of coal mine tunnels. "Apply" here means either compute large-scale configurations directly, or use scaling laws to extrapolate results obtained on smaller scales. The values that need to be extrapolated are distances to DDT and the duration of maximum pressure pulse at the end wall.

In the materials presented above in Task 1.3 and in publications [34-36], we described the results of computations of distances to DDT, L_{DDT}, in methane-air mixtures contained in channels with periodic obstacles and in channels with rock rubble. For channels with periodic obstacles, we also computed the distances to formation of the shock-flame complex, L_{SF}, that provide an important measure of a destructive potential for a particular reactive mixture and channel geometry, especially for high blockage ratios, where L_{SF} can be significantly shorter than L_{DDT}. We varied the channel size d, and computed most of the cases for d up to 2.6, 3.0, or 3.2 m. Here we summarize the results that were directly computed at $d = 3$ m or extrapolated to $d = 3$ m, which is a typical size of coal mine tunnels.

For $d = 3$m, the flame evolution in channels with periodic obstacles produced DDT in the range of $L_{DDT} = 28 - 50$ m from the ignition point, depending on the blockage ratio, br, and obstacle spacing, L. The shortest $L_{DDT} = 28$ m was observed for $br = 0.3$, $L/d = 0.5$. The shortest $L_{SF} = 18$ m was observed for $br = 0.7$, $L/d = 0.5$.

For $d = 3$ m, the flame evolution in channels with rock rubble produced DDT in the range $L_{DDT} = 5 - 9$ m, depending on br. The shortest $L_{DDT} = 5$ m was observed for the channel completely filled with rocks ($br = 1$). These L_{DDT} are significantly shorter than in channels with periodic obstacles. In application to coal mine tunnels, this means that the volume of explosive mixture required for a detonation to form is smaller in tunnels with rock rubble.

Once a detonation develops, it continues to propagate through the channel until it burns all the reactive mixture. Detonation pressures are essentially the same for all channels with stoichiometric mixtures, though the exact shape of the pressure pulse at the end wall of the channel depends on the channel size and geometry. For example, Figure 13 shows typical pressure histories at the end wall computed for three channels with periodic obstacles. All channels have the same size, $d = 3$ m, but differ by the obstacle height and spacing. In all cases, there are two initial pressure peaks reaching ~ 50 atm and spaced at $1 - 2$ ms. The first peak is the reflection of the detonation shock from the end wall, and the second one corresponds to the reflected shock bouncing between the end wall and the last obstacle. These peaks are followed by a gradual pressure decrease with some oscillations. The average pressure drops below 10 atm after ~ 20 ms.

These typical pressure histories are observed when a detonation forms far from the end wall. If DDT occurs at a short distance, $\sim d$, from the end wall, the peak pressures at the wall are higher (up to $\sim$100 atm) because the overdriven detonation produced by the DDT event does not have enough time to weaken before the collision [33, 34]. The highest pressure peaks (up to $\sim$300 atm) are observed when the detonation forms at the collision of a strong shock-flame complex with the end wall [33, 34].

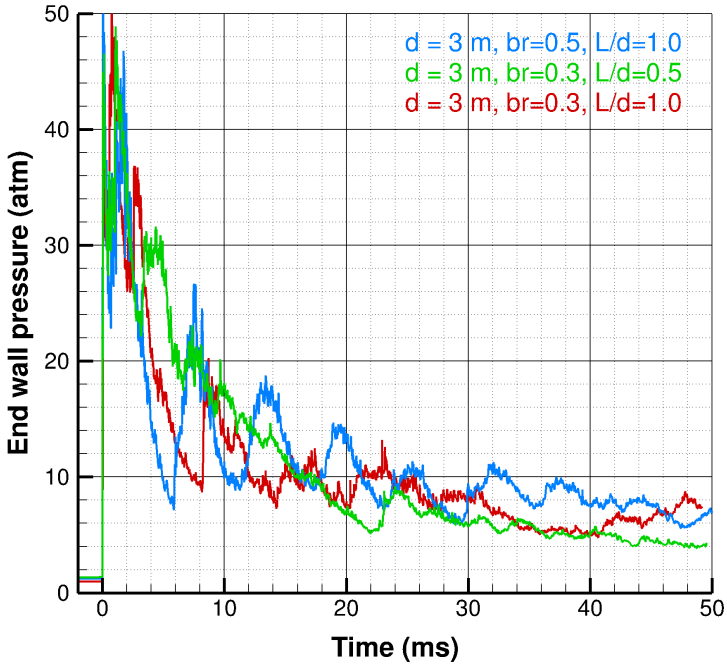

Figure 13. Pressure histories at the end wall computed for three channels with periodic obstacles: $d = 3$ m, $br = 0.5$, $L/d = 1$, $d = 3$ m, $br = 0.3$, $L/d = 0.5$, and $d = 3$ m, $br = 0.3$, $L/d = 1.0$. The averaged pressures shown are computed using pressures recorded at four different locations along the end wall. Zero at the time axis corresponds to the shock collision with the end wall.

Objective 2: To predict the development of explosions for methane-air mixtures blended with higher hydrocarbons: C_2H_6 and C_3H_8.

Task 2.1. Develop and calibrate chemical-diffusion models applicable to both deflagrations and detonations in methane-air mixtures with additives (one additive at a time). The model must reproduce distances to DDT measured in experiments with additives (if available), and a qualitative behavior of flames and detonations in mixtures observed in experiments.

The procedure for finding an appropriate chemical-diffusion model (CDM) for use in complex numerical simulations of flames and detonations was developed in the previous Alpha Foundation project and has now been published in a technical journal [37]. That paper shows how to use a genetic algorithm and an optimization routine to find optimal values of model parameters for methane-air mixtures.

The fundamental idea of the CDM is to postulate a functional form of the reaction rate, here as

$$\frac{dY}{dt} = \dot{\omega} = -\rho A Y e^{-E_a/RT} \tag{1}$$

where Y is the fuel mass fraction, t is time, A is the pre-exponential factor, ρ is the fluid density, E_a is the activation energy, R is the universal gas constant, and T is the fluid temperature. Then,

we find values of the set of variables $\{\gamma, A, E_a, q, \kappa_o, M_w\}$ such that the calculated set of flame and detonation properties $\{T_b, T_{cv}, S_l, x_{ft}, D_{CJ}, x_d\}$ match their prespecified target values. Definitions of these model parameters and flame and detonation properties are given in Tables 3 and 4.

Table 3. Reaction Parameters

Parameter	Definition
γ	Ratio of specific heats
A	Pre-exponential factor
E_a	Activation energy
q	Chemical heat release
κ_0	Thermal conductivity coefficient
M_w	Molecular weight

Table 4. Flame and Detonation Properties

Properties	Definition
T_b	Adiabatic flame temperature
T_{cv}	Equilibrium temperature at constant volume
S_l	Laminar flame speed
x_{ft}	Laminar flame thickness
D_{CJ}	Chapman-Jouguet detonation velocity
x_d	Detonation half-reaction thickness

For the prior Alpha Foundation project, the CDM was calibrated for stoichiometric methane-air, and then later it was expanded to account for varying equivalence ratios of methane [38, 39]. As part of this current project, the CDM was calibrated for methane-air mixtures containing various small percentages of ethane or propane, two hydrocarbons often found in small quantities in natural gas. This is a necessary precursor for evaluating the effects of these hydrocarbons on flame acceleration and DDT, which has been accomplished in Task 2.2

The prespecified flame properties as a function of the percentage of additive (ethane or propane) in the mixture were determined from chemical equilibrium and one-dimensional flame calculations using the Cantera [40] and the NASA Gordon-McBride [41] codes. The prespecified detonation properties for these mixtures were determined from one-dimensional detonation calculations using the CalTech Shock and Detonation Toolbox [42] based on Cantera. All of the calculations of the prespecified properties were based on the detailed chemical reaction mechanism GRI3.0 [43] which is designed to model natural gas combustion and includes 53 species and 325 reactions. When the optimal reaction parameters are used in Eq. (1) and coupled to the reactive Navier-Stokes equations, the resulting flame and detonation properties (T_b, T_{cv}, S_l, x_{ft}, D_{CJ}, x_d) closely match their prespecified target values.

(a) Methane-air mixtures with ethane impurities

We have found reaction parameters for stoichiometric methane-ethane-air mixtures in which the blended fuel contains 1%, 2%, 4%, 6% and 8% ethane, by volume. Figures 14 and 15 show the prespecified flame properties and detonation properties, respectively, as a function of the percentage of ethane in the fuel.

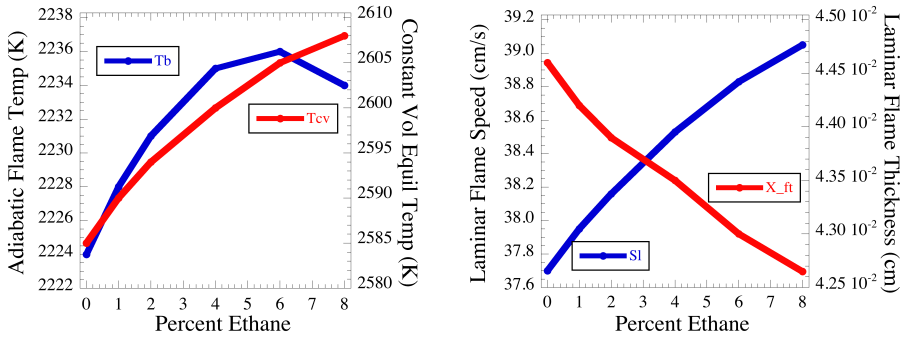

Figure 14. Left: Adiabatic flame temperature and constant volume equilibrium temperature as a function of ethane concentration. Right: Laminar flame speed and thickness as a function of ethane concentration.

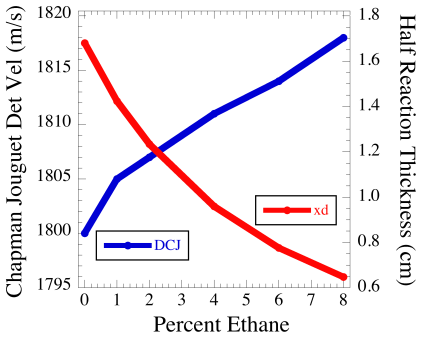

Figure 15. CJ detonation velocity and half reaction thickness as a function of ethane concentration.

The genetic algorithm optimization procedure was then carried out for each mixture. Table 5 shows the resulting optimal reaction parameters for each mixture, while Table 6 shows the target flame and detonation properties and indicates how well the genetic algorithm reproduced the target values.

Table 5. Model Parameters for Stoichiometric Methane-Air Mixtures Containing Ethane Impurities

Percent ethane, by volume	γ	E_a/RT	A (cm^3/g-s)	qM_w/RT	k_0 ($g/s\text{-}cm\text{-}K^{0.7}$)	M_w (g/mole)
1%	1.19	81.38	$1.26x10^{14}$	41.36	$6.88x10^{-6}$	27.29
2%	1.19	84.10	$1.95x10^{14}$	40.39	$6.94x10^{-6}$	27.34
4%	1.19	81.59	$1.32x10^{14}$	40.50	$6.90x10^{-6}$	27.42
6%	1.19	78.95	$8.82x10^{13}$	40.64	$6.81x10^{-6}$	27.27
8%	1.19	79.89	$1.05x10^{14}$	39.92	6.81x10-6	27.30

Table 6. Flame and Detonation Properties Computed for Stoichiometric Methane-Air Mixtures with Ethane Impurities

0% ethane	Calculated	Target
D_{CJ} (m/s)	1800	1800
S_l (cm/s)	37.7	37.7
x_{ft} (cm)	0.0448	0.0446
T_b (K)	2229	2224
x_d (cm)	1.67	1.68
T_{cv} (K)	2579	2585

1% ethane	Calculated	Target
D_{CJ} (m/s)	1806	1805
S_l (cm/s)	37.8	37.95
x_{ft} (cm)	0.0443	0.0442
T_b (K)	2229	2228
x_d (cm)	1.423	1.424
T_{cv} (K)	2588	2589

2% ethane	Calculated	Target
D_{CJ} (m/s)	1810	1807
S_l (cm/s)	38.09	38.16
x_{ft} (cm)	0.0441	0.0439
T_b (K)	2228	2231
x_d (cm)	1.235	1.23
T_{cv} (K)	2597	2593

4% ethane	Calculated	Target
D_{CJ} (m/s)	1809	1811
S_l (cm/s)	38.56	38.53
x_{ft} (cm)	0.0434	0.0435
T_b (K)	2232	2235
x_d (cm)	0.9602	0.9596
T_{cv} (K)	2602	2600

6% ethane	Calculated	Target
D_{CJ} (m/s)	1815	1815
S_l (cm/s)	38.83	38.84
x_{ft} (cm)	0.0431	0.0431
T_b (K)	2235	2236
x_d (cm)	0.7761	0.7758
T_{cv} (K)	2604	2605

8% ethane	Calculated	Target
D_{CJ} (m/s)	1817	1818
S_l (cm/s)	39.07	39.05
x_{ft} (cm)	0.0426	0.0427
T_b (K)	2233	2234
x_d (cm)	0.6475	0.6472
T_{cv} (K)	2609	2608

(b) Methane-propane mixtures

We have also found reaction parameters for stoichiometric methane-propane-air mixtures in which the blended fuel contains 1%, 2%, 4%, 6% and 8% propane, by volume. Figures 16 and 17 show the prespecified flame properties and detonation properties, respectively, as a function of the percentage of propane in the fuel.

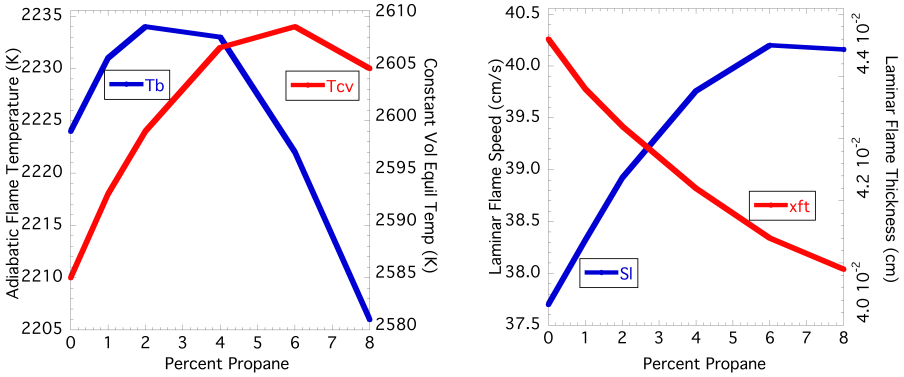

Figure 16. Left: Adiabatic flame temperature and constant volume equilibrium temperature as a function of propane concentration. Right: Laminar flame speed and thickness as a function of propane concentration.

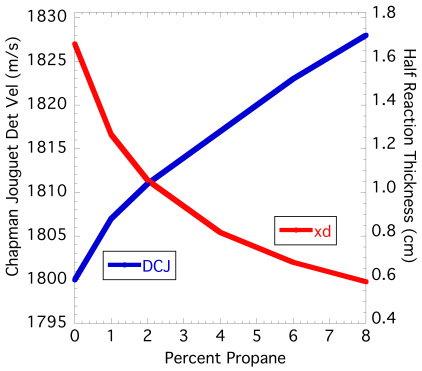

Figure 17. CJ detonation velocity and half reaction thickness as a function of propane concentration.

The genetic algorithm optimization procedure was then carried out for each mixture. Table 7 shows the resulting optimal reaction parameters for each mixture, while Table 8 shows the target flame and detonation properties and indicates how well the genetic algorithm reproduced the target values.

Table 7. Model Parameters for Stoichiometric Methane-Air Mixtures Containing Propane Impurities

Percent propane, by volume	γ	E_a/RT	A (cm^3/g-s)	qM_w/RT	k_0 (g/s-cm-$K^{0.7}$)	M_w (g/mole)
1%	1.19	88.65	4.139×10^{14}	39.51	7.009×10^{-6}	27.37
2%	1.19	82.70	1.573×10^{14}	40.57	7.024×10^{-6}	27.50
4%	1.19	81.78	1.453×10^{14}	40.20	6.860×10^{-6}	27.11
6%	1.20	82.54	1.720×10^{14}	39.41	6.881×10^{-6}	27.38
8%	1.21	91.77	8.225×10^{14}	37.03	6.890×10^{-6}	27.13

Table 8. Flame and Detonation Properties Computed for Stoichiometric Methane-Air Mixtures with Propane Impurities

0% propane	Calculated	Target
D_{CJ} (m/s)	1800	1800
S_l (cm/s)	37.7	37.7
x_{ft} (cm)	0.0448	0.0446
T_b (K)	2229	2224
x_d (cm)	1.67	1.68
T_{cv} (K)	2579	2585

1% propane	Calculated	Target
D_{CJ} (m/s)	1813	1807
S_l (cm/s)	38.63	38.32
x_{ft} (cm)	0.0434	0.0438
T_b (K)	2225	2231
x_d (cm)	1.276	1.265
T_{cv} (K)	2601	2593

2% propane	Calculated	Target
D_{CJ} (m/s)	1807	1811
S_l (cm/s)	39.03	38.92
x_{ft} (cm)	0.0435	0.0432
T_b (K)	2234	2234
x_d (cm)	1.056	1.056
T_{cv} (K)	2603	2599

4% propane	Calculated	Target
D_{CJ} (m/s)	1822	1817
S_l (cm/s)	39.81	39.76
x_{ft} (cm)	0.0442	0.0422
T_b (K)	2234	2233
x_d (cm)	0.817	0.817
T_{cv} (K)	2606	2607

6% propane	Calculated	Target
D_{CJ} (m/s)	1813	1823
S_l (cm/s)	39.98	40.20
x_{ft} (cm)	0.0417	0.0414
T_b (K)	2225	2222
x_d (cm)	0.678	0.680
T_{cv} (K)	2604	2609

8% propane	Calculated	Target
D_{CJ} (m/s)	1828	1828
S_l (cm/s)	40.17	40.16
x_{ft} (cm)	0.0409	0.0409
T_b (K)	2206	2206
x_d (cm)	0.591	0.591
T_{cv} (K)	2605	2605

Task 2.2. Compute flame acceleration and DDT in mixtures with additives for single obstructed channels, and compare the results to pure methane-air mixtures. The comparison should show whether additives can reduce the distances to DDT, and how this effect depends of the additive concentration. The computations and analysis will be performed for small scales.

Task 2.3. If the results of 2.2 show that additives can significantly reduce distances to DDT, extrapolate these distances to larger scales typical of coal mines.

We computed flame acceleration and DDT in obstructed channels filled with methane-ethane-air or methane-propane-air mixtures using the reactive fluid dynamics code FAST and calibrated model parameters from Task 2.1. The channel geometry is the same as shown in Fig. 1 with $br = 0.3$, $L/d = 1$. The flame was ignited at the closed end of the channel and accelerated as the flow interacted with obstacles. The resulting L_{DDT} as functions of additive concentrations are summarized in Figure 18 for d =17.4, 52 and 100 cm.

Multiple points for each concentration in Fig 18 were computed for slightly different initial temperatures within 0.05 K intervals to allow us to evaluate the stochastic response. Though the results show a significant scatter, the addition of both ethane and propane reduced L_{DDT} in the 17.4 cm channel by about the same 15% at concentration 2%, and by 20% at concentration 8%. For larger channels, the scatter increases, and the data do not show a clear trend.

Then we tried to estimate the effect of propane concentration on L_{DDT} for channels completely filled with arrays of obstacles that model rock rubble. We used the blockage ratio $br = 1$ that corresponds to a channel completely filled with rocks, as shown in Fig. 19. We varied the propane concentration between 0 and 8%, and the channel height d between 32 and 128 cm. For the 32 cm channel, we also computed DDT for mixtures with ethane. The resulting L_{DDT}, summarized in Fig. 20, increases with d, but shows no systematic effect of the additional propane or ethane. This effect may exist, but if so, it is less than the stochastic variations of L_{DDT}, which are 5-10% for most of the cases shown in Figure 20.

This is consistent with the fact that small ethane or propane concentrations have little effect on the laminar flame speed and flame temperature in the resulting mixture, as shown in Tables 6 and 8. For example, increasing the propane concentration from 0 to 8% increases the laminar flame speed S_l of the stoichiometric methane-propane-air mixture by 6.5% while the flame temperature T_b varies by about 1%. Since S_l and T_b control the flame evolution for the most part of L_{DDT} in obstructed channels, the resulting effect of propane concentration on L_{DDT} is small. On the other hand, the same increase in propane concentration from 0 to 8% decreases the length of the reaction zone in a detonation wave x_d by a factor of 2.8. This should facilitate the shock-induced ignition that is involved at the last stages of DDT, but these last stages are very short compared to the preceding flame evolution in obstructed channels, and thus they have little effect on L_{DDT}.

We thus conclude that up to 8% concentrations of ethane or propane in blended methane-air mixtures have no practical effect on the distances to DDT in obstructed channels. The estimated L_{DDT} for blended mixtures are essentially the same as for pure methane-air described in the previous section.

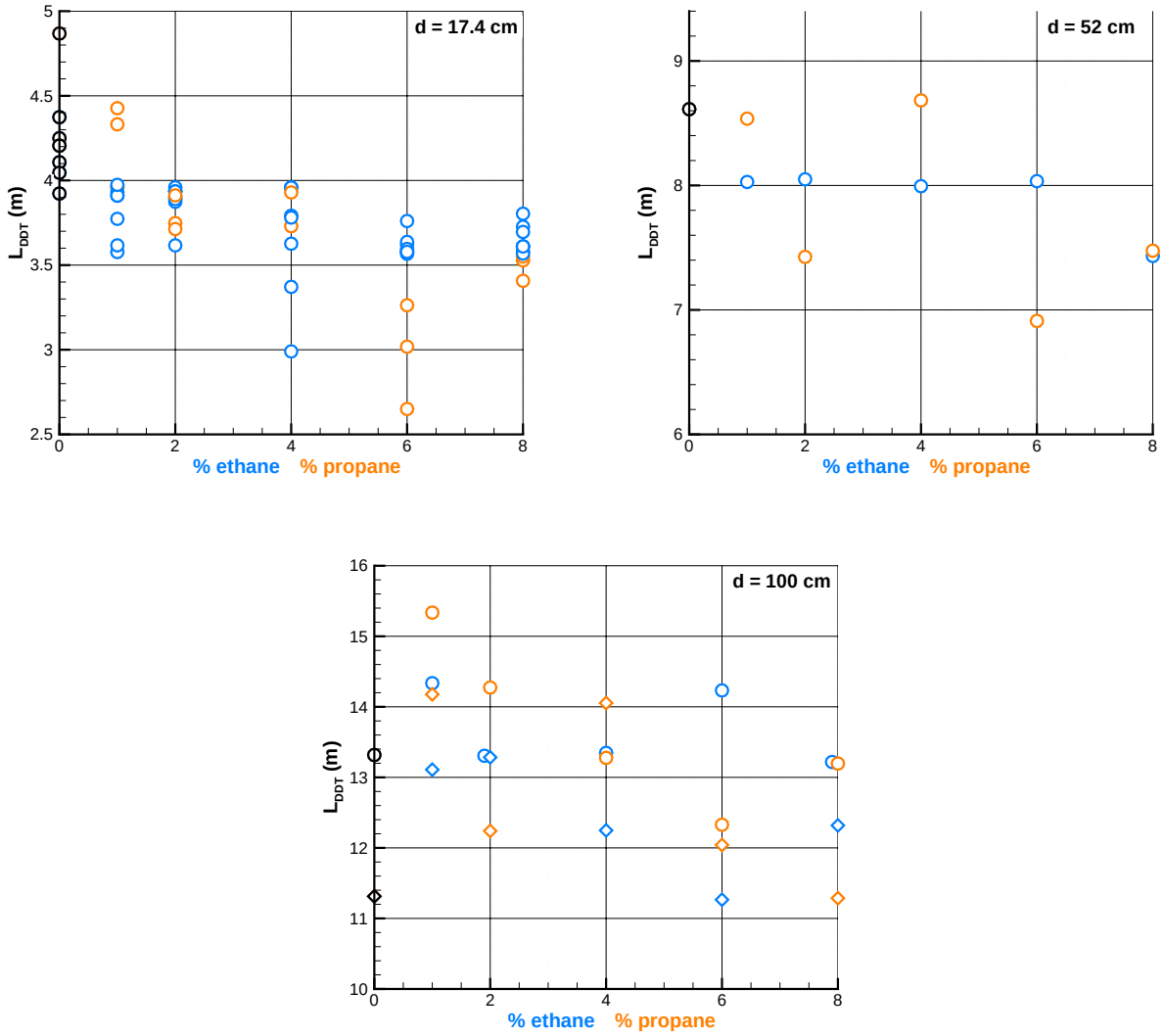

Figure 18. Computed distances to DDT for methane-ethane-air and methane-propane-air mixtures. $d = 17.4$ cm (left), 52 cm (right), and 100 cm (bottom). $br = 0.3$, $L/d = 1$. $dx_{min} = 0.03$ cm (circles) and 0.015 cm (diamonds).

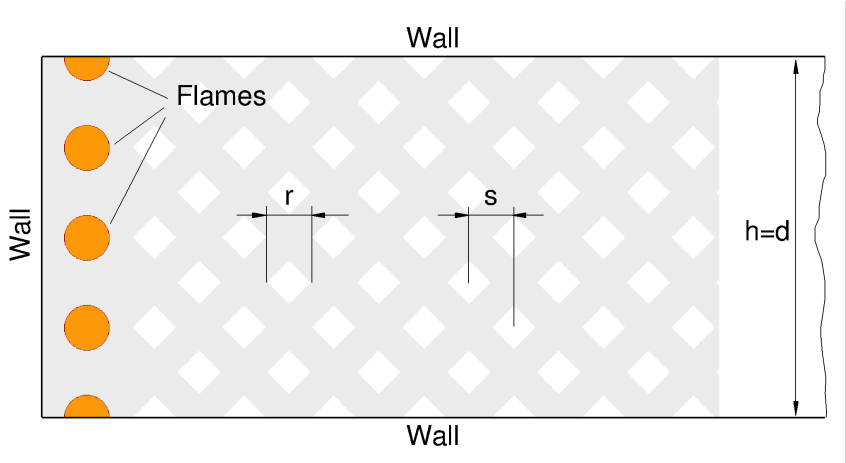

Figure 19. Computational setup for a channel completely filled with rock rubble ($br = 1$) . The channel and obstacle array extend to the right for many d as needed for a detonation to develop.

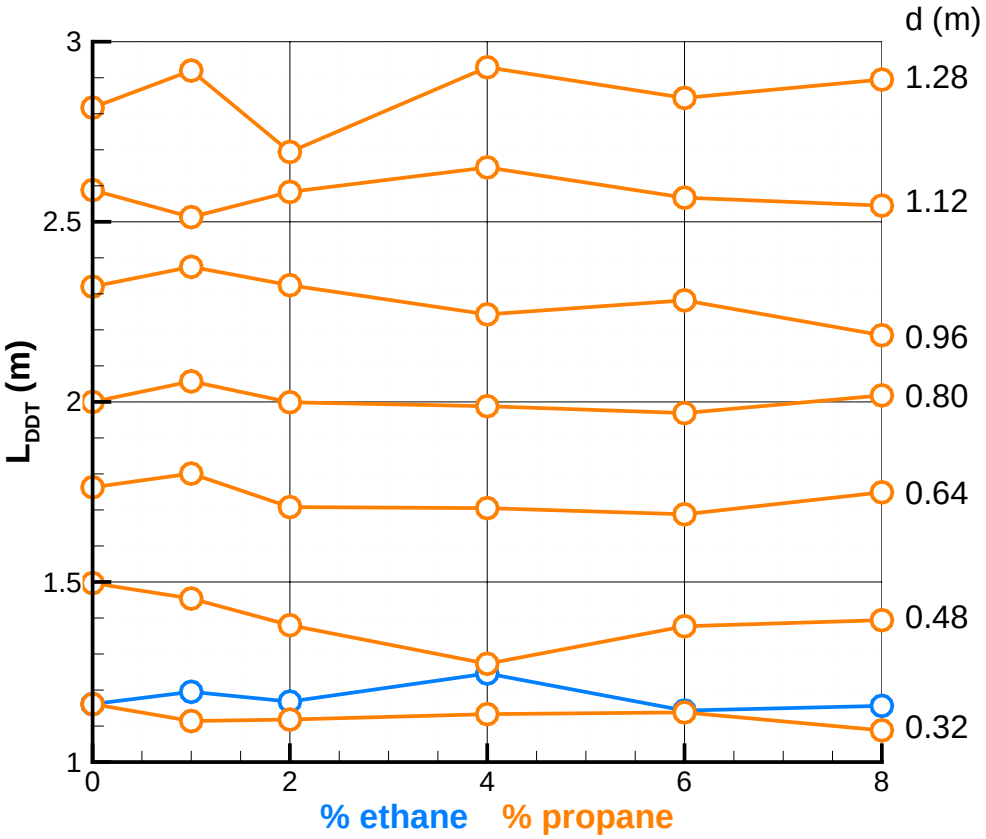

Figure 20. Computed distances to DDT for methane-ethane-air and methane-propane-air mixtures in channels filled with rock rubble. $br = 1$, $s = r$, $dx_{min} = 1/16$ cm, $dx_{max} = 1/8$ cm.

Objective 3: To analyze the specifications for protective seal design.

Task 3.1. Compute the effect of gas explosions on protective seals by modifying the downstream boundary used in calculations for objectives 1 and 2 to simulate a solid wall. Each simulation will record the pressure history at the end wall. The computed pressure histories will be compared to the current MSHA criteria for seal design.

We computed the effect of gas explosions on protective seals by placing a solid wall at the downstream end of the channel and recording pressure histories at this wall. Typical pressure histories produced by detonations colliding with the end wall for $d = 3$ m are shown in Figure 13, and these were discussed above. These pressure histories are very similar for all cases with stoichiometric mixtures where detonations form at a distance greater than a few d from the end wall. These include both pure methane-air and blended mixtures since the small additives have little effect on the chemical energy released in a detonation wave, and therefore on the detonation velocity and pressure.

Protective walls (seals) that separate active and abandoned areas in coal mines are designed to protect workers from accidental gas and coal dust explosions in abandoned areas. Therefore, the seals are expected to withstand expected possible explosion pressures that depend on particular conditions in a coal mine. In 2007, NIOSH [6] recommended to select the design pressures for protective seals using the flowchart shown in Figure 21.

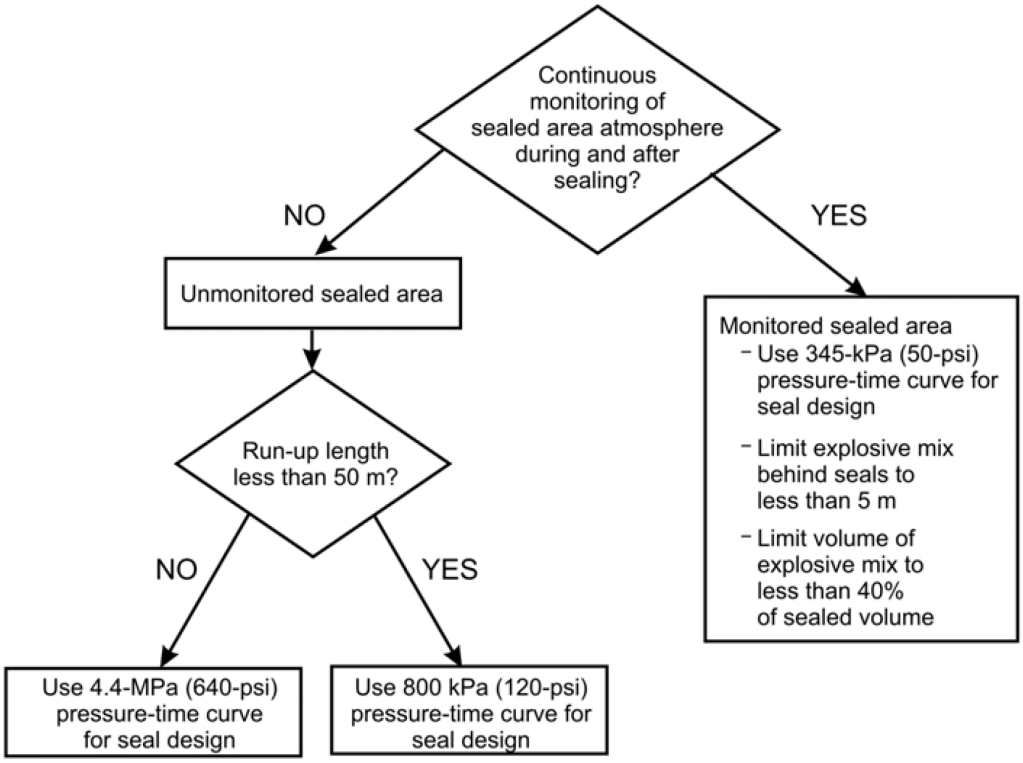

Figure 21. Flowchart for selecting design pressures for protective seals in coal mines [6].

On this flowchart, the worst-case scenarios that we consider correspond to the lower left rectangle that applies to unmonitored sealed areas where explosive mixtures can form and cover areas up to 50 m long (run-up length). For these conditions, NIOSH recommended seals that withstand a static pressure of 640 psi (43.5 atm). This pressure is consistent with reflected detonations and $\sim$ 50 atm pressure peaks at the end wall shown in Fig. 13. (Short pressure pulses can slightly exceed the static design pressure without damaging the seal). In our simulations, however, the distances to DDT in $d = 3$ m channels are significantly shorter than 50 m. As discussed above, the minimum L_{DDT} is 28 m for channels with periodic obstacles, and 5 m for channels filled with rocks. Since the sealed areas can be easily filled with rock rubble (gob or other areas with a collapsed roof), we would expect detonations for areas longer than 5 m. We would use this as the detonation threshold instead of 50 m in Fig. 21.

The actual MSHA regulations released in 2008 [5] differ form the NIOSH recommendations [6]. In particular, the run-up length criterion in Fig. 21 was replaced with a set of conditions that include the formation of homogeneous methane-air mixtures with concentrations within detonability limits, a possibility of pressure piling, and the likelihood of a detonation. If any of these conditions applies, then the seal should be designed for pressures above 120 psi (8.2 atm), but the maximum pressure should be calculated for each particular case. The 640 psi design pressure is not explicitly included in MSHA regulations, but it will appear if the conditions point to a possible detonation and the required calculations produce a reflected detonation.

Our results show that the possibility and the destructive potential of detonations in underground coal mines should not be underestimated. Detonations in near-stoichiometric methane-air mixtures contained in obstructed areas can develop quickly on the scales as short as 5 m, and produce reflected-shock pressures $\sim$50 atm (735 psi). These detonations cannot be contained by the standard 50 psi or 120 psi seals that are designed to stop relatively slow deflagrations. In areas with a high risk of detonations, the seals should be designed to withstand the static pressure of at least 640 psi, as previously recommended by NIOSH.

Objective 4: An important, new addition to this project will be the availability of data taken at the new experimental detonation test facility at the Colorado School of Mines (CSM). Throughout the project, simulation results will be compared to their experimental measurements, as data are relevant to the proposed become available research.

CSM is developing a new facility that consists of a 71 cm diameter tube that has several sections. It can be extended up to 34 m, or length-to-diameter ratio up to 48. This tube length largely exceeds the distance to DDT observed in our simulations of flame propagation in channels with rock rubble filled with stoichiometric methane-air mixtures. We agreed on the parameters of the first series of experiments that will allow the CSM team to test the facility and the sound suppression system, and also allow us to start validating our numerical models. The planned experiments will include layers of 4-6 inch rocks placed at the bottom of the tube. The tube length and the resulting explosion pressures will be increased gradually.

There were a series of meetings held with personnel from CSM and UMD-NRL to initiate and plan the collaboration. A history of the most important meetings is given below.

September 14, 2019

Dr. Elaine Oran visited CSM and talked to Dr. Gregory Bogin and others at the Edgar Mine. This was an introductory session for Dr. Oran on the capabilities of Edgar Mine. In particular, they discussed the construction of the new facility and the noise it creates on firing.

February 4, 2019

This was a more formal telecon including Dr. Elaine Oran, Dr. Carolyn Kaplan, Dr. Vadim Gamezo, and Christian Bachman representing the UMD-NRL team, and Dr. Gregory Bogin, Dr. Jürgen Brune, Dr. Richard Gilmore, Casey DeRosa, Nikhil Tiwari, and Hamilton Pinheiro representing the CSM team. Dr. Bogin gave a detailed summary of progress to date, along with the timeline for the CSM project. Their experiments showed that for smaller tubes, there was enhanced flame acceleration when rubble was put close to the ignition point, rather than further down the channel.

Based on what Dr. Bogin showed, both in terms of their plans and the results they have to date, we saw good points of collaboration that should lead to interesting and useful results.

- The first is comparing experimental (CSM) and numerical (UMD-NRL) results for flame acceleration and DDT in channels partially filled with rock rubble. The simulations and experiments can vary the height and porosity of the rock layer, as well as the rock sizes. Comparisons could be made of flame speeds, shock pressures, and distances to DDT.
- The second is an exchange of chemical models. It would be useful to use our chemical model in their simulations
- CSM is using turbulence models in their simulations. UMD-NRL are resolving most of the relevant scales of the turbulent flow. We can address the question: What is the effect of turbulence models on their calculations?
- We will provide the CSM team with mixture compositions that can be used in both experiments and simulations. The experimental and numerical results then can be compared to each other and analyzed for the effects of turbulence on flame acceleration.

For Task 1.2, we computed flame acceleration and DDT for single channels of various heights partially filled with rock rubble. We varied the height and porosity of the rock layer, as well as the rock sizes, with the objective of comparing the results with experimental data produced at CSM. The results of simulations of flame propagation and DDT in channels with rock rubble led to recommendations for the initial set of experiments at CSM.

August 28, 2019

A telecon was held to discuss the coordination between the experimental and numerical teams. Participating personnel included Dr. Elaine Oran, Dr. Carolyn Kaplan, Dr. Vadim Gamezo, and Logan Kunka from the UMD-NRL group and Dr. Gregory Bogin, Dr. Jürgen Brune, and Richard Gilmore from CSM. Dr. Bogin, reported that the new test facility at CSM is almost ready, and should be available for experiments this fall.

September, 2020

According to Dr. Bogin, the CSM team is currently performing the safety testing and certification of the experimental facility using relatively slow flames in a smooth tube without obstructions. The length of the tube section filled with the methane-air mixture is gradually increased to allow the sound mitigation system to be tested for moderate pressures. Experiments with rocks are expected later this year. Although our Alpha computational project will be finished when these CSM experiments begin, we plan to be involved and use our computational results to advise the experimental team.

It was highly unfortunate that a combination of weather and the Covid-19 pandemic made it impossible for CSM to provide data on the timeline expected.

5. Publications

Numerical Tools for Mitigation of Methane Explosions in Coal Mines, V.N. Gamezo, E.S. Oran, C.R. Kaplan, R.W., Houim, H. Xiao, W. and Zheng,
NRL Memorandum Report NRL/MR/604319-9833, 2019.

Effect of Rock-Dust on Suppression of Coal-Dust Entrainment by Shock Waves S. Lai, R.W. Houim, E.S. Oran, Proceedings of the 27th International Colloquium on the Dynamics of Explosions and Reactive Systems (ICDERS), Beijing, 2019.

Flame Acceleration and Transition to Detonation in Methane-Air Mixtures with Composition Gradients, W. Zheng, C.R. Kaplan, R.W. Houim, E.S. Oran, and H. Xiao, 27th Proceedings of the 27th International Colloquium on the Dynamics of Explosions and Reactive Systems (ICDERS), 2019.

Role of Reactivity Gradients in the Survival, Decay and Reignition of Methane-Air Detonations in Large Channels, P. Honhar, C.R. Kaplan, R.W. Houim, and E.S. Oran, *Combustion and Flame*, 222, 152-169. 2020.

Flame Acceleration and DDT in Large-Scale Obstructed Channels Filled with Methane-Air Mixtures, V.N. Gamezo, C.L. Bachman, E.S. Oran, to appear, *Proceedings of the Combustion Institute*, 2020.

Towards Scaling Laws for DDT in Obstructed Channels, E.S. Oran and V.N. Gamezo, *Progress in Scale Modeling*, 1, Article 4, 2020. https://uknowledge.uky.edu/psmij/vol1/iss1/4

Simulation of Flame Acceleration and DDT in Methane-Air Mixtures Containing Trace Hydrocarbon Impurities, L.N. Kunka. X. Lu, C.L. Bachman, C.R. Kaplan, V.N. Gamezo, E.S. Oran, in preparation for *Combustion and Flame*, to be submitted Fall 2020.

Presentations

Flame Acceleration and Transition to Detonation in Methane-Air Mixtures with Composition Gradients, W. Zheng, C.R. Kaplan, R.W. Houim, E.S. Oran, and H. Xiao, 27th International Colloquium on the Dynamics of Explosions and Reactive Systems (ICDERS), Beijing, July 2019.

Numerical Simulation of Flame Acceleration and Detonations in Coal Mines. L.N. Kunka, E.S. Oran, Sandia National Laboratories, Albuquerque, NM, October 2019.

Effects of Scale on Flame Acceleration and DDT in Obstructed Channels, V.N. Gamezo, C.L.. Bachman, and E.S. Oran, AIAA SciTech Forum, American Institute of Aeronautics and Astronautics, Orlando FL, January 2020.

Numerical Simulation of Methane-Air DDT in Channels Containing Trace Amounts of Impurities, L.N. Kunka, C.R. Kaplan, and E.S. Oran, 23rd Annual Process Safety International Symposium, Texas A&M, October 2020.

Calibrating Chemical-Diusive Model for Multidimensional Combustion Properties, X. Lu, C.R. Kaplan, and E.S. Oran, Meeting of the American Physical Society, Division of Fluid Dynamics, Chicago, IL, November 2020,

Numerical simulations of flame acceleration and DDT in natural gas: the effect of trace propane and ethane. L.N. Kunka. X. Lu, C.R. Kaplan, V.N. Gamezo, E.S. Oran. Meeting of the Division of Fluid Dynamics, American Physical Society, Chicago, IL, November 2020.

Flame Acceleration and DDT in Large-Scale Obstructed Channels Filled with Methane-Air Mixtures, V.N. Gamezo, C.L. Bachman, E.S. Oran, to be presented at the 38th International Symposium, on Combustion, Adelaide, Australia, January, 2021.

Invited Presentations

Turbulence and Transitions in Reactive Flows, E.S. Oran, F.M. Global, Norwood, MA, March 2018.

Turbulence and Transitions in Reactive Flows, E.S. Oran, Frank J. Molina Lecture, Texas A&M, College Station, TX, March 2018.

The Beauty of Turbulence and Transitions in Reactive Flow, E.S. Oran, Lighthill Lecture, Imperial College, London, UK, June 2018.

The Beauty of Turbulence and Transitions in Reactive Flow, E.S. Oran, Hong Kong University of Science and Technology, November 2018.

Turbulence and Transition in High-Speed Reactive Flows, E.S. Oran, Theodore on Karman Lecture, 59th Israel Annual Conference on Aerospace Sciences, Tel Aviv, Israel, March 2019.

Turbulence and Transitions in Reactive Flows, E.S. Oran, 8th International Symposium on the Physics of Fluids, Xian, China, June 2019.

Update on the Hunt for The Origin of DDT in Gas-Phase Reactive Flows. E.S. Oran, Department of Aerospace Engineering, Texas A&M University, Department Seminar, October 2019.

Mechanisms of Deflagration-to-Detonation Transition in Large-Scale Explosions, E.S. Oran, 2019 International Symposium in honor of Dr. Sam Mannan, Mary K. OConnor Process Safety Center, Texas A&M University, October 2019.

6. Conclusions and Impact

a. General Conclusions

An overriding conclusion and result of this and the predecessor Alpha Foundation project is that the capability of using numerical simulations to compute flame acceleration and the transition to detonation is now at the state where simulations can be used to evaluate the danger of explosions in coal mines and guide decisions on the design of protective seals.

An important choice in these studies was to consider worst-case scenarios. Thus we focused on obstructed channels filled with *stoichiometric* methane-air mixtures and varied the channel height and types of blockage. The objective was to compute the flame evolution to the point where strong shocks and possibly detonations appear. We considered two types of obstructions: periodic obstacles placed on channel walls, and rock rubble that partially fills the channel.

For channels with periodic obstacles, the distance where a shock-flame complex is formed, L_{SF}, and the location at which a detonation occurs, L_{DDT}, were computed as functions of channel height d, blockage ratio br, and obstacle spacing L for the ranges $d = 0.174 - 3$ m, $br = 0.3 - 0.7$, and $L/d = 0.5 - 1.5$.

The results of simulations show two main effects. On one hand, the increase of br and decrease of L/d promote the flame acceleration and reduce L_{SF} and L_{DDT}. On the other hand, some configurations with higher br and smaller L/d prevent the detonation development, even though local detonations may form in isolated pockets of unburned material between obstacles. These local detonations, however, appear behind the leading edge of the flame and cannot spread downstream. As a result, the leading shock and the flame never merge, and continue to propagate as a quasi-steady-state shock-flame complex. This complex is characterized by a strong shock followed by a thick compressed layer of unburned material, and a turbulent flame. The collision of this complex with the end wall or other solid structures generates high pressures and strong reflected shocks that can ignite a detonation. This detonation propagates in a shock-compressed material and results in extremely high pressures at the wall that exceed wall pressures produced by a regular detonation by a factor of $5 - 10$. Thus, both L_{DDT} and L_{SF} are important measures of the destructive potential for a particular reactive mixture and channel geometry. The distance L_{SF} is especially relevant for channels with high br where L_{SF} can be significantly shorter than L_{DDT}.

Deriving scaling laws that show how L_{DDT} and L_{SF} change with system parameters was an important part of this program. The analysis of the computational data for fixed br and L/d shows that both L_{DDT} and L_{SF} increase with d such that L_{DDT}/d and L_{SF}/d decrease. For the maximum computed channel height of 3 m, the minimum $L_{DDT} = 28$ m ($L_{DDT}/d \approx 9$) was observed for $br = 0.3$, $L/d = 0.5$, and the minimum $L_{SF} = 18$ m ($L_{SF}/d \approx 6$) was extrapolated for $br = 0.7$, $L/d = 0.5$. These distances are relevant for coal mine tunnels that have typical sizes $\sim$3 m and can contain explosive methane-air mixtures.

For channels with rock rubble, we computed L_{DDT} as functions of channel height up to $d = 3.2$ m for blockage ratios in the range $br = 0.4375 - 1$. The results show that L_{DDT} increases and L_{DDT}/d decreases with d. Both L_{DDT} and L_{DDT}/d decrease with the increasing blockage ratio, and reach the minimum when the channel is completely filled with rocks ($br = 1$). For $d = 3$ m typical of coal mine tunnels, L_{DDT} reaches $8 - 9$ m for $br = 0.4375$, and 5-5.5 m for $br = 1$. This corresponds to $L_{DDT}/d \approx 3$ for $br = 0.4375$, and $L_{DDT}/d \approx 1.8$ for $br = 1$. These DDT lengths are significantly shorter than values computed for channels with periodic obstacles, but

they correspond to worst-case scenarios with relatively loose rock layers that may not be typical for realistic coal mine environments.

Since natural gas is not 100% pure methane, but includes small percentages of higher hydrocarbons, mainly ethane and propane, we studied effects of these impurities on flame acceleration and DDT. We derived chemical-diffusive models for stoichiometric methane-ethane-air and methane-propane-air mixtures assuming that the fuel contains 1-8% of ethane or propane. These models were used in extensive series of simulations of the flame acceleration and DDT in channels with periodic obstacles or rock rubble. The somewhat surprising result was that up to 8% concentrations of ethane or propane in blended mixtures have no practical effect on the distances to DDT in obstructed channels. The estimated L_{DDT} for blended mixtures are basically the same as for pure methane-air mixtures.

This is consistent with the fact that small ethane or propane concentrations have little effect on the laminar flame speed S_l and flame temperature T_b in the resulting mixture. Since S_l and T_b control the flame evolution for the most part of L_{DDT} in obstructed channels, the resulting effect of ethane or propane concentration on L_{DDT} is small. On the other hand, the same increase in propane concentration from 0 to 8% decreases the length of the reaction zone in a detonation wave x_d by a factor of 2.8. This should facilitate the shock-induced ignition that is involved at the last stages of DDT, but these last stages are very short compared to the preceding flame evolution in obstructed channels, and thus have little effect on L_{DDT}.

b. Impact

The work performed in this project has impact through two specific types of contributions. The first is to mining safety, which was the immediate goal of this project. The second is to combustion sciences and computational approaches to complex reactive flow problems.

There are several different types of environments in a coal mine in which methane explosions may occur. One kind is the mined out regions that are sealed off and contain considerable amounts of fallen rock. Another could be long tunnels with possible crosscuts, and with rubble or equipment on the floor. Channels with any amount of blockage can occur in any of these environments on scales from centimeters for interconnected voids inside piles of rubble, to meters for unobstructed or partially obstructed tunnels. In this sense, channel geometries of all sizes up to the typical tunnel height $\sim$3 m, and any blockage ratios are relevant for studies of flame acceleration and DDT in coal mines.

On scales $\sim$3 m typical of coal mines, the minimum distances to DDT in channels filled with rock rubble are about 5 m, which is 5-6 times shorter than in channels with periodic obstacles, and 10 times shorter than the 50 m condition proposed by NIOSH. Reflected detonation pressures in closed channels are consistent with the NIOSH-recommended 640 psi design pressure for the protective seals. Small additions of ethane or propane to methane-air mixtures have practically no effect on the distance to DDT.

In terms of combustion science and computational approaches, we have extended the capabilities of the Chemical-Diffusive Model so that it now can describe mixtures of fuels. Prior work extended this model to gradients in composition, and this led to work showing that it can also accurately describe diffusion flames.

The simulations showed the role of upstream DDT events in unreacted material trapped among obstacles for maintaining the leading shock-flame complex, a highly destructive wave that can persist

for a substantial period of time. The distance at which the shock-flame complex forms provides an important measure of the destructive potential, especially for channels with high blockage ratios where self-sustained detonations may not form at all, or may develop at a significantly greater distance than the shock-flame complex.

Interactions with the CSM team set up a group effort that resulted in recommendations for the first set of experiments with rock rubble planned at the new CSM facility this fall.

7. Future Work

Future work on numerical simulation of methane-air explosions should include:

– Extensions of the computations and analysis to include dust particles, both inert and coal, dispersed in the mine atmosphere and on large scales. Examination of how the presence of dust affects flame acceleration, DDT, resulting pressures, and scaling laws.

– Development of a simplified, inexpensive radiation transport model that accounts for radiation effects in the presence of dust.

– Integration of simulations with an experimental program, for example, at the Colorado school of Mines. Numerical results will help to plan experiments that will produce more data for model validation.

– Selected three-dimensional simulations to evaluate the effects of large-scale turbulence on flame acceleration, DDT and scaling laws.

– Application of the developed predictive capabilities for the analysis and development of explosion mitigation devices, such as active barriers

– Creation of a summary document explaining where we stand on this problem.

8. References

[1] Mining Disasters. New York Times, Dec. 6, 2011.
https://www.nytimes.com/topic/subject/mining-disasters

[2] "All Mining Disasters, 1839 to present." NIOSH, 2011.
http://www.cdc.gov/niosh/mining/statistics/content/allminingdisasters.html

[3] Historical Data on Mine Disasters in the United States. MSHA.
http://www.msha.gov/MSHAINFO/FactSheets/MSHAFCT8.HTM

[4] R.K. Eckhoff. *Explosion Hazards in the Process Industries*. Gulf Publishing Company, Houston, Texas, 2005. 457p. ISBN: 0-9765113-4-7.

[5] 30 CFR Part 75. Sealing of Abandoned Areas; Final Rule. Fed. Reg. 73:21182-21209 (2008).
http://www.msha.gov/regs/fedreg/final/2008finl/08-1152.pdf

[6] R.K. Zipf, Jr., M.J. Sapko, J.F. Brune. *Explosion Pressure Design Criteria for New Seals in U.S. Coal Mines*. NIOSH Publication No. 2007–144, Information Circular 9500, 2007 July, 1-76. http://www.cdc.gov/niosh/mining/UserFiles/works/pdfs/2007-144.pdf

[7] K. Takahashi, K. Watanabe. Advanced Numerical Simulation of Gas Explosion for Assessing the Safety of Oil and Gas Plant. Chapter 18 in *Numerical Simulations - Examples and Applications in Computational Fluid Dynamics*. Ed. by L. Angermann, InTech, 2010, 450 p. ISBN 978-953-307-153-4. http://www.intechopen.com/books/numerical-simulations-examples-and-applications-in-computational-fluid-dynamics

[8] G.W. McMahon, J.R. Britt, J.L. O'Daniel, L.K. Davis, R.E. Walker. *CFD Study and Structural Analysis of the Sago Mine Accident*. US Army Corps of Engineers, Engineer Research and Development Center, Geotechnical and Structures Laboratory, 2007, ERDC/GSL TR-06-X, 138 pp. https://arlweb.msha.gov/sagomine/CFDSagoReport.pdf

[9] A.M. Khokhlov, E.S. Oran, Numerical simulation of detonation initiation in a flame brush: The role of hot spots, *Combustion and Flame* 119 (1999) 400–416.

[10] V.N. Gamezo, T. Ogawa, E.S. Oran, Numerical simulations of flame propagation and DDT in obstructed channels filled with hydrogen-air mixture, *Proceedings of the Combustion Institute* 31 (2007) 2463–2471.

[11] A.Y. Poludnenko, T.A. Gardiner, E.S. Oran, Spontaneous transition of turbulent flames to detonations in unconfined media, *Phys. Rev. Lett.* 107 (2011) 054501.

[12] R.W. Houim, E.S. Oran. Numerical simulation of dilute and dense layered coal-dust explosions. *Proceedings of the Combustion Institute* 35 (2015) 2083–2090. http://dx.doi.org/10.1016/j.proci.2014.06.032

[13] Modeling Natural Gas Explosions for Coal Mine Safety, NIOSH-NRL Interagency Agreement #08FED898342. www.cdc.gov/niosh/mining/researchprogram/contracts/iag_08FED898342.html

[14] D.A. Kessler, V.N. Gamezo, E.S. Oran, Simulations of flame acceleration and deflagration-to-detonation transitions in methane-air systems, *Combustion and Flame* 157 (2010) 2063–2077.

[15] V.N. Gamezo, E.S. Oran. Analysis of Efficiency of Passive Blast Attenuators for Reactive Gas Mixtures. AIAA SciTech, Kissimmee, Florida, 8-12 January 2018. AIAA 2018-1418.

[16] D.A. Kessler, V.N. Gamezo, E.S. Oran, Multilevel detonation cell structures in methane-air mixtures, *Proceedings of the Combustion Institute* 33 (2011) 2211–2218.

[17] D.A. Kessler, V.N. Gamezo, E.S. Oran. Gas-Phase Detonation Propagation in Composition Gradients, *Phil. Trans. R. Soc. Lond.* A 370 (2012) 567–596.

[18] E.S. Oran, V.N. Gamezo, D.A. Kessler. *Deflagrations, Detonations, and the Deflagration-to-Detonation Transition in Methane-Air Mixtures*. NRL Memorandum Report 6400-11-9332, 2011. http://www.dtic.mil/get-tr-doc/pdf?AD=ADA544015

[19] V. Molkov. Fundamentals of Hydrogen Safety Engineering II. 2012. 232 p. ISBN: 978-87-403-0279-0. http://bookboon.com/en/fundamentals-of-hydrogen-safety-engineering-ii-ebook.

[20] A. Silde, I. Lindholm, On Detonation Dynamics in Hydrogen-Air-Steam Mixtures: Theory and Application to Olkiluoto Reactor Building. Nordic Nuclear Safety Research, Report NKS-9, 2000, ISBN 87-7893-058-8, http://www.nks.org/en/nks_reports/view_document.htm?id=111010111119689.

[21] A. Silde, R. Redlinger. Three-dimensional Simulation of Hydrogen Detonations in the Olkiluoto BWR Reactor. Nordic Nuclear Safety Research, Report NKS-27, ISBN: 87-7893-078-2. http://www.nks.org/en/nks_reports/view_document.htm?id=111010111119721.

[22] M. Kuznetsov, A. Lelyakin and W. Breitung, Numerical Simulation of Radiolysis Gas Detonations in a BWR Exhaust Pipe and Mechanical Response of the Piping to the Detonation Pressure Loads. Chapter 19, *Numerical Simulations – Examples and Applications in Computational Fluid Dynamics*, edited by L. Angermann, InTech, 2010, 450 p. ISBN 978-953-307-153-4. http://www.intechopen.com/books/numerical-simulations-examples-and-applications-in-computational-fluid-dynamics

[23] L.J. Spadaccini, M.B. Colket III. Ignition Delay Characteristics of Methane Fuels. Progress in Energy and Combustion Science 20, 431460, 1994.

[24] N. Lamoureux, C.E. Paillard, Natural gas ignition delay times behind reflected shock waves: Application to modelling and safety. Shock Waves 13, 5768, 2003.

[25] A.G. Kim, The Composition of Coalbed Gas. U.S. Bureau of Mines, Washington, 1973, Report of investigation 7762.

[26] M.A. Trevits, G.L. Finfinger, Coalbed Gas: An Analysis of the Relationship Between Gas Content, Gas Composition and Mine Emissions. Proceedings of the 4th U.S. Mine Ventilation Symposium. University of California, Berkley, CA 1989.

[27] C.K. Westbrook, W.J. Pit, Effects of Propane on Ignition of Methane-Ethane-Air Mixtures. Combustion Science and Technology 33, 315319, 1983.

[28] D.D. Rice, Composition and origins of coalbed gas, in: B.E. Law, D.D. Rice, (Eds.), Hydrocarbons from Coal, AAPG Studies in Geology #38, Tulsa, OK, 1993, pp. 159184.

[29] J.L. Clayton. Geochemistry of coalbed gas A review. International Journal of Coal Geology 35, 159173, 1998.

[30] M. Niemann. Stable Isotope Systematics of Coalbed Methane. Ph.D. Thesis, 2006. University of Victoria, Canada.

[31] T. Harvey, J. Gray. The Unconventional Hydrocarbon Resources of Britains Onshore Basins Coalbed Methane (CBM). U.K. Department of Energy and Climate Change, 2013.

[32] N. Ripepi, K. Louk, J. Amante, C. Schlosser, X. Tang, E. Gilliland. Determining Coalbed Methane Production and Composition from Individual Stacked Coal Seams in a Multi-Zone Completed Gas Well. Energies 10, 1533, 2017.

[33] E.S. Oran, V.N. Gamezo, C.R. Kaplan, R. Houim, H. Xiao, W. Zheng. Numerical Tools for Mitigation of Methane Explosions in Coal Mines. NRL Memorandum Report. 2019. NRL/MR/604319-9833.

[34] V.N. Gamezo, C.L. Bachman, ES. Oran. Effects of Scale of Flame Acceleration and DDT in Obstructed Channels. AIAA SciTech meeting, 6-10 January, 2020, Orlando, Florida. AIAA 2020-0443.

[35] V. N. Gamezo, C.L. Bachman, E.S. Oran. Flame Acceleration and DDT in Large-Scale Obstructed Channels Filled with Methane-Air Mixtures. Proceedings of the Combustion Institute, 38, 2020.

[36] V.N. Gamezo, C.L. Bachman, E.S. Oran. Towards scaling laws for DDT in obstructed channels. Progress in Scale Modeling, an International Journal Vol. 1 (2020) 2428.

[37] C.R. Kaplan, A. Ozgen, E.S. Oran. Chemical-diffusive models for flame acceleration and transition-to-detonation: genetic algorithm and optimisation procedure, *Combustion Theory and Modelling* 23 (2019) 66.

[38] W. Zheng, C.R. Kaplan, E.S. Oran. Flame acceleration and transition to detonation: Effects of a composition gradient in a mixture of methane and air, *Proceedings of the Combustion Institute* 37 (2019) 3521.

[39] P. Honhar, C.R. Kaplan, R.W. Houim, E.S. Oran, Role of reactivity gradients in the survival, decay and reignition of methane-air detonations in large channels, *Combustion and Flame* 222 (2020) 152.

[40] D.G. Goodwin, H.K. Moffat, and R.L. Speth, Cantera: An object-oriented software toolkit for chemical kinetics, thermodynamics, and transport processes, 2016. Version 2.1. Available at http://www.cantera.org.

[41] S. Gordon and B. McBride, Computer program for calculation of complex chemical equilibrium composition, rocket performance, incident and reflected shocks and Chapman-Jouguet detonation, NASA SP-273, NASA Lewis Research Center, Cleveland, 1976.

[42] Explosion Dynamics Laboratory, California Institute of Technology, Shock & Detonation Toolbox for Cantera 2.1 (2015).

[43] G.P. Smith, D.M. Golden, M. Frenklach, N.W. Moriarty, B. Eiteneer, M. Goldenberg, C.T. Bowman, R.K. Hanson, S. Song, W.C. Gardiner Jr., V.V. Lissianski, and Z. Qin, GRI-MECH 3.0, Available at http://www.me.berkeley.edu/gri mech/.